

Evaluation of the deposition, translocation and pathological response of brake dust with and without added chrysotile in comparison to crocidolite asbestos following short-term inhalation: Interim results

David M. Bernstein ^{a,*}, Rick Rogers ^b, Rosalina Sepulveda ^b, Peter Kunzendorf ^c, Bernd Bellmann ^{d,1}, Heinrich Ernst ^d, James I. Phillips ^{e,f}

^a Consultant in Toxicology, 1208 Geneva, Switzerland

^b Rogers Imaging, Needham, MA 02494, USA

^c GSA Gesellschaft für Schadstoffanalytik mbH, D-40882 Ratingen, Germany

^d Fraunhofer Institute for Toxicology and Experimental Medicine, D-30625 Hannover, Germany

^e National Institute for Occupational Health, National Health Laboratory Service, South Africa

^f Department of Biomedical Technology, Faculty of Health Sciences, University of Johannesburg, South Africa

ARTICLE INFO

Article history:

Received 14 November 2013

Revised 15 January 2014

Accepted 18 January 2014

Available online 28 January 2014

Keywords:

Brake dust

Chrysotile

Amphibole asbestos

Inhalation toxicology

Pathology

Lung/pleura

ABSTRACT

Chrysotile has been frequently used in the past in manufacturing brakes and continues to be used in brakes in many countries. This study was designed to provide an understanding of the biokinetics and potential toxicology following inhalation of brake dust following short term exposure in rats. The deposition, translocation and pathological response of brake dust derived from brake pads manufactured with chrysotile were evaluated in comparison to the amphibole, crocidolite asbestos. Rats were exposed by inhalation 6 h/day for 5 days to either brake dust obtained by sanding of brake-drums manufactured with chrysotile, a mixture of chrysotile and the brake dust or crocidolite asbestos. No significant pathological response was observed at any time point in either the brake dust or chrysotile/brake dust exposure groups. The long chrysotile fibers ($>20\ \mu\text{m}$) cleared quickly with $T_{1/2}$ estimated as 30 and 33 days, respectively in the brake dust and the chrysotile/brake dust exposure groups. In contrast, the long crocidolite fibers had a $T_{1/2} > 1000$ days and initiated a rapid inflammatory response in the lung following exposure resulting in a 5-fold increase in fibrotic response within 91 days. These results provide support that brake dust derived from chrysotile containing brake drums would not initiate a pathological response in the lung following short term inhalation.

© 2014 The Authors. Published by Elsevier Inc. Open access under [CC BY-NC-ND license](https://creativecommons.org/licenses/by-nc-nd/4.0/).

Introduction

The use of braking systems for automobiles had evolved from the earliest automobiles. Initially, friction materials were used that consisted of materials like camel hair, cotton belting, elm wood and cotton based materials impregnated with different ingredients (Harper, 1998; Paustenbach et al., 2004). These initial materials, however, were limited in their ability to withstand heat and control speed. From the early 1900s chrysotile fibers were found to be an effective replacement for these earlier materials. The chrysotile fibers maintained their integrity under higher temperatures which allowed the driver to

brake at increased vehicle speeds (Harper, 1998). Because of these unique characteristics, chrysotile became the material of choice for vehicle brakes.

With the use of chrysotile, researchers began to investigate the degree of exposure to the fibers experienced by mechanics servicing the brakes. Short duration activities, such as removal of brake-wear debris (e.g., brake dust) from brake assemblies (often using compressed air or a dry brush) and the machining of brake linings (often by grinding or bevelling the lining surfaces to provide a better fit with the drum) have been reported to produce occupational dust exposures (Richter et al., 2009).

While many publications have reported that brakes that have used chrysotile are not related to disease when taking into consideration confounders such as smoking and other exposures (Butnor et al., 2003; Finley et al., 2012; Laden et al., 2004; Marsh et al., 2011; Paustenbach et al., 2004); others continue to report a relationship with mesothelioma (Dodson and Hamner, 2012; Freeman and Kohles, 2012; Lemen, 2004). Although chrysotile containing brakes are not manufactured in the United States they can be imported, and they are still manufactured and used in many countries. The U.S. Census

* Corresponding author at: 40 chemin de la Petite-Boissière, 1208 Geneva, Switzerland. Fax: +41 22 735 1463.

E-mail addresses: davidb@itox.ch (D.M. Bernstein), rrogers5@yahoo.com (R. Rogers), Peter.Kunzendorf@GSA-Ratingen.de (P. Kunzendorf), Heinrich.ernst@item.fraunhofer.de (H. Ernst), jim.phillips@nioh.nhls.ac.za (J.I. Phillips).

¹ Deceased.

Bureau indicated that companies in the United States imported asbestos-containing brake pads and linings from Brazil, China, Colombia, India, and Mexico in 2012 (Harmonized Tariff Schedule code 6813.20.00.10 and 6813.20.00.20, www.census.gov/foreign-trade/). In addition, the United Nations Commodity Trade Database indicates that Indonesia, Kazakhstan, Malaysia, Russia, and Ukraine also may have exported asbestos-containing brakes in 2012 (Harmonized Tariff Schedule code 681320, comtrade.un.org/db/). The potential for exposure to chrysotile containing brake dust remains.

This study was designed to evaluate the hypothesis of whether brake dust from chrysotile containing brake drums will produce a pathological response following short term exposure in rats. Brake dust has not been previously evaluated in animal studies.

The exposure design was based upon a frequently used protocol for the evaluation of fiber biopersistence and short term toxicity (EUR, 18748 EN, 1999; ILSI, 2005) which has been used for evaluating a wide variety of synthetic and natural mineral fibers. This design is based upon the evaluation of fiber lung clearance using lung digestion procedures. In addition to criteria specified in these protocols, the current study includes histopathological examination of the lungs, the evaluation of fiber localization and number in the lung and pleura using confocal microscopy, and the quantification of fibrosis (collagen) in the lung and pleura through confocal microscopy (Antonini et al., 1999). This is the first such study in which the fibrotic response following fiber inhalation has been quantified using confocal microscopy.

The interim results presented here on the lung provide a basis for evaluating the biopersistence and pulmonary response of both brake dust alone and brake dust combined with added chrysotile in comparison to crocidolite asbestos following short term exposure through 91 days post exposure. The procedures used for evaluation of the pleural space included examination of the diaphragm as a parietal pleural tissue and the *in situ* examination of the lungs and pleural space obtained from freeze-substituted tissue in deep frozen rats, however, due to the large amount of data these results will be published separately.

The brake dust used in this study was obtained from commercial brake pads that were produced using chrysotile as one of the components by sanding the surfaces of the brake pads using a commercial brake pad sanding machine with the dust collected on filters. The sanded brake dust consists largely of binders with some chrysotile. To achieve the recommended aerosol concentration referred to in the above protocol (>100 f/cm³ longer than 20 μ m; this length category being related to pathogenesis) two brake dust exposure groups were included, one with brake dust alone and the other with brake dust with added chrysotile. Also included in this study was a comparative positive control group using crocidolite asbestos exposed at a similar concentration of fibers longer than 20 μ m. This group was unique in that the crocidolite asbestos was obtained directly from South Africa without prior selection or milling as has been performed for most previously studied samples.

Methods

The aerosol generation/exposure, in-life and pathology phases of this study were performed by the Fraunhofer Institute for Toxicology and Experimental Medicine (Hannover, Germany) in compliance with the Principles of Good Laboratory Practice (German Chemicals Act §19a, Appendix 1, July 02, 2008, Federal Law Gazette I, No. 28, p. 1146) and the German animal protection law (Tierschutzgesetz of May 18, 2006, German Federal Law Gazette I, page 1206, 1313). The fiber counting and sizing was performed by Gesellschaft für Schadstoffanalytik mbH (Ratingen, Germany). The confocal microscopy was performed by Rogers Imaging (Needham, Massachusetts, USA).

Brake dust preparation

The brake dust was produced directly from asbestos-containing friction products (automotive drum brake shoes) by the RJ LeeGroup Ltd. (Monroeville, PA, USA). The brake shoes were obtained from Davies McFarland & Carroll (Pittsburgh, PA). The shoes were designed to fit the drum brakes of mid-1960's Chevrolet Impala model cars. These shoes were labeled either "BX MN FF" or "BX MG FF" (manufactured by Bendix). Two of the shoes had never been installed in vehicles; the other shoes that were used in this project were installed and operated in vehicles for a two week period. The friction material was evaluated and found to contain approximately 30% (by area) chrysotile asbestos (analyzed in accordance with EPA 600/R-93/116). No amphibole asbestos minerals have been observed in any of the aerosol or lung samples from these brake shoes or in the added chrysotile used in this study.

The brake dust was produced by grinding the brake shoes using a commercial AMMCO arc grinder (Model 8000, S/N 24788) with a modified dust collection system. The arc grinder is a motorized sander that is swept across the surface of the brake shoe with the dust collected on an attached 8 × 10 inch quartz micro-fiber filter that was used in place of a collection bag. A Tisch high volume air sampler sampling pump (Tisch Environmental Inc., Ohio, USA) was used following the filter to provide uniform sampling suction over the course of the grinding operation. All brake dust preparation took place at the RJ LeeGroup facility in a room equipped with an Aramsco Comanche® HEPA ventilation unit (Model 55011) with a nominal flowrate of 1800 cfm (50 m³/min).

The composition of the brake dust was determined quantitatively using inductively coupled plasma mass spectrometry (ICP-MS) following the German norm DIN EN ISO 17294-2 (INDIKATOR GmbH, Wuppertal, Germany). The results are presented in the Supplementary data, Tables S-1 and S-2.

Chrysotile

The chrysotile fiber used in this study had the mineralogical grade of 5R04 according to the Canadian chrysotile asbestos classification (Cossette and Delvaux, 1979). The chrysotile sample was chosen based upon an evaluation of which chrysotile grade was ordered or supplied for use in brake manufacturing in a random search of 67 formulations dating from 1964 to 1986. Chrysotile grade 5R04 was used most frequently (25% of the samples) and was chosen for use in the study. All of the grade 5R04 chrysotile in these samples was supplied by Johns-Manville. The sample used in this study was obtained directly from Mine Jeffery Canada (formerly the Johns-Manville Mine).

The 5R04 sample received had some large bundles of fibers. To separate these bundles into respirable fibers without significantly reducing the fiber length, the bulk material was passed one time for 60 s through a table top rotating blade mill to break up the large bundles and then was passed once to separate the fibers through the Cyclotec Sample Mill (FOSS Tecator, Denmark) which rolls the sample against the inner circumference and then separates the fibrils through a fine mesh screen.

Crocidolite asbestos

The crocidolite asbestos used previously in animal studies has been largely either the Union for International Cancer Control (UICC) or US National Institute of Environmental Health Sciences (NIEHS) prepared crocidolite. Both of these samples were ground extensively more than 30 years ago using large scale industrial mills resulting in size distribution not typical of the commercial product (Bernstein et al., 2013). In this study, a crocidolite asbestos sample from the Voorspoed mine in South Africa was obtained from the National Institute of Occupational Health — NIOH, South Africa. This mine is located in Limpopo Province which at the time when mining took place was called Transvaal Province.

The chemical compositions of chrysotile, a serpentine asbestos, and crocidolite, an amphibole asbestos, have been described previously (Shedd, 1985; Virta, 2002).

Experimental design

The experimental design of the study is illustrated in the flowchart in Fig. 1. All end points were analyzed for each group with the exception that lung digestion was not performed in the control group on days 1, 2 and 7 in order to limit animal use.

Animal exposure

Groups of laboratory rats (Groups 1, 2, 3 and 4) were exposed for 6 h per day for 5 days to:

Group 1: Filtered air (negative control Group)

Group 2: Brake dust powder mixed with chrysotile 5R04.

Group 3: Brake dust powder.

Group 4: Crocidolite asbestos.

For groups 2 and 4, the exposure concentrations were set based upon the number of fibers longer than $20 \mu\text{m}/\text{cm}^3$. In group 2, the chrysotile concentration was increased over that recommended by the EC Biopersistence Protocol (Bernstein and Riego-Sintes, 1999) of 100 fibers $L > 20 \mu\text{m}/\text{cm}^3$ due to the tendency of chrysotile to clump (this was minimized through the use of the cyclone, see below). Group 3 was included as a comparative exposure of the brake dust particulate material (with a relatively low aerosol concentration of chrysotile fibers) using a similar gravimetric exposure concentration as the brake dust component of group 2. A negative control group 1 was exposed in a similar fashion to filtered air.

Weanling (8–10 weeks old at exposure) male Wistar rats (CrI: Wi(Han), Specific Pathogen Free from Charles River Deutschland, Sulzfeld, Germany) were used. The rats were exposed by flow-past nose-only exposure for 6 h/day for a period of 5 consecutive days.

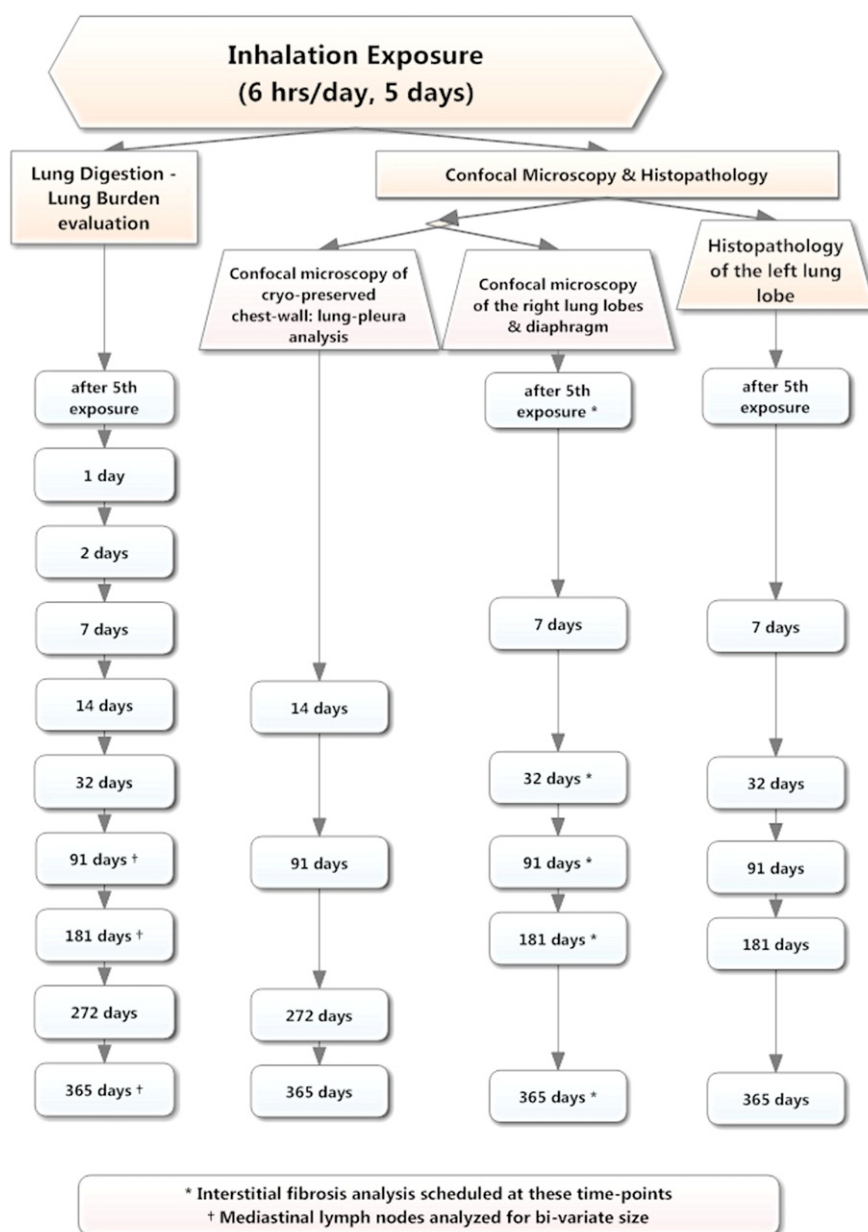


Fig. 1. Flowchart of the experimental design of the analyses in the study.

Exposure system

The fiber aerosol generation system (Model CR 3020, CR Equipments, Switzerland) was designed to loft the bulk fibers without breaking, grinding or contaminating the fibers (Bernstein et al., 1994). The animals were exposed using stainless steel flow-past nose-only inhalation exposure systems with 16 animals per level. This system was derived from Cannon et al. (1983) and is different from conventional nose-only exposure systems in that fresh fiber aerosol is supplied to each animal individually and exhaled air is immediately exhausted. The exposure units were placed in separate ventilated chambers connected to the animal room to avoid cross contamination between the groups.

For group 2 (chrysotile fiber 5R04 mixed with brake dust powder), a fiber aerosol was generated from chrysotile fiber 5R04 and separately a dust aerosol from the brake dust using individual rotating brush aerosol generators (Fig. 2). The fiber aerosol generator used was followed by a 500 mL pyrex glass cyclone to assist in the elimination of any remaining fiber bundles from the aerosol. The brake dust aerosol generator was followed by a micronising jet mill to reduce the particle size to be rat respirable. Following each generator, in-line ^{63}Ni charge neutralisers reduced the electrostatic charge from fibers and particulate material in the generated aerosols. Following the charge neutralizers, the fiber and powder aerosols were mixed through a Y-piece connection and then delivered directly into the nose-only flow-past exposure chamber.

The group 3 brake dust aerosol was generated using only the 'powder aerosol generator' as shown in bottom left of Fig. 2.

The group 4 crocidolite asbestos aerosol was generated using only the 'fiber aerosol generator' as shown in the top left of Fig. 2. A pre-study technical trial revealed stronger electrostatic properties of the crocidolite fiber aerosol which resulted in losses in the transfer tubing. To achieve a similar degree of neutralization with similar fiber transfer

efficiency as with the chrysotile an electronic charge neutraliser at the brush head of the aerosol generator (WEKO Model AP230, Weitmann & Konrad GmbH, Germany) was used in addition to the ^{63}Ni charge neutraliser.

Exposure system monitoring

The aerosol concentration was monitored continuously using an aerosol photometer developed by Fraunhofer ITEM. Actual concentrations were measured in the breathing zone of the animals as described below. The temperature and the relative humidity of the exposure atmosphere were monitored continuously with data on temperature, relative humidity, and air flow rate collected by the Fraunhofer ITEM animal exposure facility computer system.

Gravimetric Determination of Aerosol Concentrations: Gravimetric determinations of aerosol concentration were performed at least once daily for each group with samples collected on a Millipore® glass fiber filter (Type 13400-25-J) for approximately 4–6 h per day.

Fiber number and size distribution of Aerosol Concentrations: Aerosol samples for bivariate analysis of fiber size distribution and counting were collected onto NUCLEOPORE® filters (PC membrane, 25 mm, pore size $0.8\ \mu\text{m}$ – SN 110.609, Whatman Ltd.) for approximately 2 h successively during each exposure period in parallel with the gravimetric sampling. For group 1 (air control) one sample per treatment day was collected over approximately 5 h per day. These samples were analyzed for bivariate fiber size distribution and counting (# fibers/ cm^3 aerosol) using analytical Scanning Electron Microscopy (SEM) with Energy Dispersive X-ray analysis (EDAX).

Counting rules for the evaluation of air and lung samples by scanning electron microscopy (Fiber/Particle Analysis and Lung Digestion): Unless otherwise specified, the basis for the evaluation using the scanning electron microscope (SEM) was WHO-Reference Methods

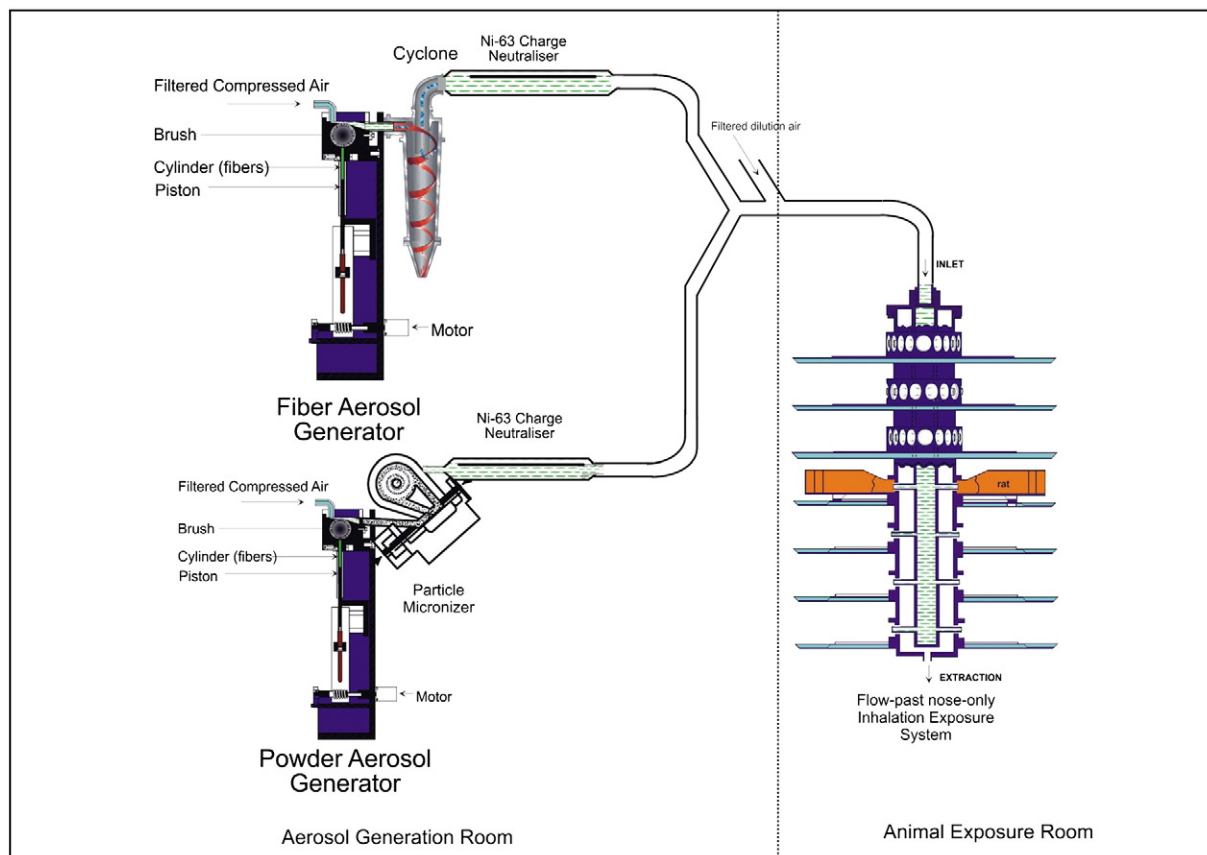


Fig. 2. Schematic diagram of the aerosol generation and exposure system used for the combined chrysotile and brake dust exposure.

for measuring airborne man made mineral fibers (MMMF) WHO (1985) and the VDI Guideline 3492 (2004).

All objects seen at the magnification of 10,000 \times (acceleration voltage 25 kV) were sized with no lower or upper limit imposed on either length or diameter. The bivariate length and diameter was recorded individually for each object measured. Fibers were defined as any object that had an aspect ratio of at least 3:1. The diameter was determined at the greatest width of the object. All other objects were considered as non-fibrous particles. Fibers with both ends in the field of view had the “weight” of one fiber (= 2 fiber ends), fibers with only one end within the field had the “weight” of a half fiber (= 1 fiber end). Fibers without any fiber end in the field of view were not counted nor measured.

The stopping rules for counting each sample were defined as follows.

Fibrous objects: The minimum numbers of fibers examined were:

- a) fibers with a length $< 5 \mu\text{m}$ = 100 fibers (200 fiber ends)
- b) fibers with a length between 5 and $20 \mu\text{m}$ = 200 fibers (400 fiber ends)
- c) fibers with a length $> 20 \mu\text{m}$ = 100 fibers (200 fiber ends)

Fields of view were examined for each length category until the defined minimum number of fibers for each length category was recorded or a maximum of 1 mm² of the filter surface was examined in case the fiber minimum number for the length category was not reached. For samples of the control group an area of 0.5 mm² of the filter was evaluated. These counting rules were based on the number of fibers per sample necessary in order to have statistical reproducibility of the means (EUR, 18748 EN, 1999). For non-fibrous objects, fields of view were examined until a total of 100 particles were recorded or the aforementioned stopping criteria for fibers were reached.

Particle Size of Dust Aerosol: The particle size of the brake dust aerosol was measured using a Marple Series 290 Cascade Impactor (TSE Systems, Germany). The impactor determines the aerodynamic particle size distributions from 0.52 to 21.3 μm .

Clinical examination and body weights

Animals were observed for mortality/morbidity and for other clinical symptoms at least once daily during the acclimatization period and the 12-month post exposure observation period and twice daily during the treatment period. Once a week, animals were examined for clinical symptoms, i.e. abnormalities concerning their general condition. This included inspection of skin, fur, eyes, visible mucous membranes, examination for patho-morphological changes (e.g. unusual breathing pattern, masses, nodules), abnormal behavior and central nervous symptoms (e.g. changes in gait, posture or grooming activity, unusual response to handling, secretion/excretion abnormalities, clonic/tonic movements, stereotypies) and/or other clinical abnormalities. Body weight was recorded weekly starting on day 1 of the acclimatization period, on days 1, 3 and 5 of the treatment period, once weekly during the first month post exposure and every second week thereafter.

Gross pathology and organ weights

Animals were anesthetized with an overdose of pentobarbital sodium (Narcoren™) and humanely killed by cutting the vena cava caudalis. The abdominal cavity was opened and the diaphragm cut carefully allowing the lungs to collapse. Heart, esophagus, upper half of trachea, thymus and lung associated lymph-nodes were sampled. The physical condition of the animals prior to euthanasia and the examination of the internal organs were recorded. Moribund animals or those found dead were necropsied as soon as possible and the findings recorded.

Tissue preparation for lung ashing, histopathology and confocal microscopy

In animals assigned to biopersistence/lung burden, the lungs and the lower half of the trachea were collected with the attached mediastinal tissue. The mediastinal tissue containing the mediastinal lymph nodes was resected and immediately inserted into appropriate labeled plastic bags and deep-frozen. All lung lobes were removed by transection of the bronchi and were weighed, inserted into appropriately labeled plastic tubes and deep frozen (-70°C) without fixation. Particular attention was given to avoid contamination of the dissected organs by fibers from the fur or deposited on dissecting instruments.

In animals assigned to lung histopathology and confocal microscopy, the lungs and the lower half of the trachea were collected with the attached mediastinal tissue. In addition, the diaphragm was collected for confocal microscopy. Macroscopic abnormalities of the lungs were recorded and the lung weight measured and recorded.

The lung lobes were dried by freeze drying (Christ, Osterode, Germany) and subjected to low temperature ashing (200-G, Plasma Technics, Kirchheim, Germany) with the ash weight calculated for each lung. An aliquot was suspended in filtered water, sonicated (Sonorex RK 510H at 35 kHz and 160 W, Bandelin, Germany) until the suspension was homogenous (~ 60 s) and filtered onto a Nuclepore filter (pore size $0.2 \mu\text{m}$). The filter was mounted on an aluminum stub and sputtered (Balzers SCD 030, Balzers Hochvakuumtechnik, Germany) with ~ 10 nm of gold.

Histopathology

The left lung lobe of each animal assigned to lung histopathology was filled with neutral buffered 4% formaldehyde solution by gentle instillation under a hydrostatic pressure of 20 cm. In addition, the mediastinal tissue containing the lymph nodes was fixed in neutral buffered 4% formaldehyde solution except at the 91, 181 and 365 day terminations as mentioned below.

The lung tissues and lymph nodes were processed, embedded in paraffin, cut at a nominal thickness of 2–4 μm and stained with hematoxylin and eosin. Special stains were used at the discretion of the pathologist. The slides were examined by light microscopy and the observations recorded.

The mediastinal lymph nodes from animals terminated at days 91, 181 and 365 were analyzed for fiber number and size. The lymph nodes were frozen, dried and plasma ashed as described for the lung lobes above and analyzed for bivariate fiber size distribution and counting by SEM.

Lung and diaphragm tissue preparation for confocal microscopy

The bronchus to the left lung was ligated, left lung removed for sampling as previously described. Right lung lobes were fixed via intratracheal instillation of modified Karnovsky's fixative (with PBS) at a hydrostatic pressure of 20 cm for at least 10 min. The trachea was then ligated and the inflated lung stored in the same fixative. Diaphragms were excised from the chest wall, pinned flat to stiff filter paper with parietal surface facing up and immersion fixed in modified Karnovsky's fixative. Specimens were then dispatched to Rogers Imaging Corporation (Needham Heights, MA, USA) for processing and analysis. Upon arrival, the fixed right lung samples were weighed, piece dissected, dehydrated, stained and embedded in Spurr epoxy (Rogers et al., 1999).

Chestwall preparation for confocal microscopy

In all animals assigned to low temperature microscopy, following termination, a gross dissection of the animal proceeded as follows: A short PE 190 tube was inserted into the trachea and fixed with silk thread. Skin surrounding the thoracic cage, the forelimbs at the brachial

plexus and the lower part of the body below the diaphragm were surgically removed. Intact chestwalls were immediately lowered into liquid nitrogen diaphragm-first over a one minute period. Frozen chestwalls were sealed in ziplock bags and stored at -80°C , then shipped to Rogers Imaging Corporation (RIC) on dry ice for freeze substitution processing.

Chest wall processing

For each chestwall a series of cross sectional slabs 4–5 mm thick were cut using a band saw. Slabs were placed on a dry ice cooled copper plate, then put into wire mesh processing baskets, labeled, and immersed by group in freeze-dry transition fluid (anhydrous methanol (75%), acetone (25%)) in 1 l cryo containers and stored at -80°C . Cyro fluids were replaced weekly for up to two months. Then specimens were stored in cryofluid at -20°C with weekly fluid replacement until solution cleared, usually after one month.

Staining and preparation of specimens for microscopic evaluation

Following freeze substitution, cross sections of chestwall were transferred to anhydrous methanol at -20°C and brought to room temperature. Chestwall slabs and lung pieces were then stained with Lucifer yellow-CH (0.0001%) (Rogers et al., 1999), infiltrated in Spurr epoxy resin then heat cured. Undisturbed surfaces of chestwall slabs were exposed within the Epoxy-embedment using a belt sander, or in the case of lung, 2 millimeter-thick sections were cut using a thin kerf rock saw blade. Exposed surfaces were polished using a diamond lapidary wheel until glass smooth.

Confocal microscopy

Confocal microscopy imaging was performed on four lung sample pieces or chestwall slabs from each animal for each time point using Sarastro 2000 or 2010 (Molecular Dynamics, Inc.) laser scanning microscopes fitted with 25 mW argon-ion lasers and an upright Zeiss Axiophot or upright Nikon or inverted Nikon Diphot2 microscopes, modified for reflected light imaging in dual channel reflected and fluorescent imaging mode. The cellular constituents and fibers (and particles) were imaged simultaneously with this arrangement with each “exposure” producing two digital images in perfect register with one another (Bernstein et al., 2010). Images were recorded through 60 \times objectives for Nikon-fitted confocal microscopes with voxel dimensions of 0.16 μm , 0.16 μm , and 0.60 μm (x, y, and z dimensions, respectively). Voxel dimensions were 0.16 μm , 0.16 μm , and 0.50 μm (x, y, and z dimensions, respectively) obtained from 63 \times objective for the Zeiss-fitted confocal microscope.

Morphometric methods for confocal analysis

Fiber load and fiber distribution. All fiber profiles in length classes of 3 μm or longer were recorded. The true length of individual fibrils was recorded if the fiber profile was oriented such that two free ends were present. Particulate material is viewed as a single spot or profile that does not deviate along X or Y axis when serial section data is scrolled up and down along the z-axis. Sampling strategies were designed to permit the determination of the number of fibers retained within the lung parenchyma and conducting airways.

Sampling strategy for parenchyma. The sampling strategy for the parenchyma has been described previously (Bernstein et al., 2010). Each volume was recorded by obtaining 25 optical sections separated by 0.5 μm along the z-axis. On average, the real-world dimensions of a volume, therefore, were 86.6 $\mu\text{m} \times 86.6 \mu\text{m} \times 13.75 \mu\text{m}$ in x, y, and z, respectively. For this phase of the study, well over 240,000 micrographs were recorded to obtain the necessary quantitative

information from this compartment. The number of fibers in each volume was counted by scrolling up and down through the depth series of images while looking for the characteristic bright points or lines which indicated a reflective or refractile particle or fiber. The number of fibers/volume of parenchyma, μm was recorded and then extrapolated to the whole lung based upon the volume of parenchyma (including airspaces).

Fibers in parenchyma were classified as occurring:

- in alveoli, alveolar ducts, or terminal bronchioles, in contact with the surface of tissue,
- in ducts or alveoli, but not in contact with tissue in the recorded volume,
- wholly or partly inside alveolar macrophages.

No fibers were observed in other parenchymal contexts.

Sampling strategy for airways. The sampling strategy for the airways has been described previously (Bernstein et al., 2010). Ten depth series (dimensions identical to parenchymal depth series) were recorded from each of 4 samples per animal, with these stacks holding, on average, 95 μm of airway wall profile each. Well over 24,000 micrographs were recorded for this phase of the study. The average airway diameter in these lungs was estimated at 300 μm , with airway volume, ca. 10% of lung volume. These numbers allow a further estimate of the length of an equivalent cylinder and its wall area, which is an estimate of the total airway wall area in the lungs. The total fiber burden in the airway compartment was estimated.

Sampling strategy for connective tissue in parenchyma

The same images used to collect quantitative measurements of pulmonary fiber load and distribution were used to measure connective tissue (Ct) present per field of view (FOV) to obtain a percentage of connective tissue occupied in a given area of lung tissue (%CT/FOV). For each FOV, the midpoint of the volume was examined and the area occupied by lung tissue was measured by adjusting the threshold detection. Fluorescent specificity imparted to the lung tissue in general, with the highest affinity to connective tissue produced images with distinct pixel intensity maps as follows; airspace was represented by pixel intensity units from 0 to 18, lung tissue occupied pixel intensities 19–180, and connective tissue (elastin and collagen) were shown in the pixel intensity range of 181–255. Overall variations of pixel intensity resulting from different depth from the block surface were adjusted by the examiner of the dataset on an individual basis by “scroll up and down” through the depth series of images. The area occupied by connective tissue was divided by the total lung tissue area from each field of view then the average %Ct/FOV was determined for each group by time point and compared. These measurements produced the fraction of connective tissue per area lung tissue for all FOVs examined.

Statistical analyses

Comparison of lung digestion and confocal methodologies was performed using concordance correlation, Lin (1989) using MedCalc Software (Version 12.7, Belgium).

The fiber clearance half-times were determined using the statistical procedures specified in the EC protocol (EUR, 18748 EN, 1999). The clearance curve was fitted to the data using nonlinear regression techniques with a single or double exponential (StatSoft, Inc. (2011). STATISTICA (data analysis software system), version 12. www.statsoft.com).

The confocal fibrotic response data was analyzed using analysis of variance (MedCalc, ver 12.7, Ostend, Belgium).

Results

Validation of the lung digestion and counting procedures

Validation of lung digestion and counting procedures is essential to the legitimacy of this type of study, although it was often absent from early studies. Such validation provides confidence that there is no significant alteration of the fiber counting and size distribution during fiber recovery. Comparative CM was used to assure that the lung digestion and SEM procedures used in this study did not affect the fiber dimensions of the chrysotile and crocidolite present in the lung (Bernstein et al., 2004).

The results of this analysis confirmed that there is a very good correlation between the length distribution as measured by the lung digestion procedure/SEM and the confocal methodology with a concordance correlation coefficient ρ_c (Lin, 1989, 2000) of 0.8384 (0.9972 with outlier removed) for group 2, 0.9956 for group 3 and 0.9823 for group 4.

Inhalation exposure

The aerosol concentrations and the size distributions of the fibers of all groups are shown in Table 1. The aerosol concentrations of groups 2 (chrysotile and brake dust) and 4 (crocidolite asbestos) were set based upon the number of fibers/cm³ longer than 20 μ m. Group 3 (brake dust alone) was included as a comparative exposure of the brake dust particulate material (with the relatively low concentration of chrysotile fibers present) with groups 2 and 3 having similar gravimetric concentrations of brake dust. The difference between the total gravimetric concentration in group 2 (3.48 mg/m³) compared to group 3 (1.52 mg/m³) was largely due to the gravimetric concentration of the chrysotile aerosol added to group 2. The mean gravimetric concentration for group 4 (crocidolite asbestos) was 6.34 mg/m³ which was a result of the crocidolite fibers having a larger diameter than the chrysotile.

Bivariate length and diameter distributions of the exposure aerosols

The bivariate length and diameter size distributions of the chrysotile and brake dust, brake dust and crocidolite aerosol are shown in Fig. 3. As mentioned above, all measurements were made at the position of the animal's nose in the exposure system. The fiber distribution in the chrysotile and brake dust aerosol included a larger number of shorter fibers with 84% less than 5 μ m. For those fibers longer than 20 μ m there was a mean of 189 fibers/cm³ ranging from 20 to 160 μ m in length. As summarized in Fig. 4, 99% of the long fibers were less than 1 μ m in diameter (rat-respirable) with 95% less than 0.4 μ m in diameter.

The crocidolite-exposure atmosphere had considerably fewer short fibers with 66% less than 5 μ m. For those fibers longer than 20 μ m there was a mean of 93 fibers/cm³ ranging in length from 20 to 190 μ m. 88% of the long fibers were less than 1 μ m in diameter (rat-respirable) with 21% of the fibers less than 0.4 μ m in diameter.

In the brake dust exposure group there were fewer chrysotile fibers present without the added chrysotile with a mean of 3 fibers longer than 20 μ m/cm³. These longer fibers ranged in length from 20 to 140 μ m with 90% less than 1 μ m in diameter (rat respirable) with 63% of the fibers less than 0.4 μ m in diameter.

SEM photomicrographs of the aerosol from each exposure group atmosphere are shown in the Supplementary data, Figs. S1–S6.

Lung fiber burden (from the lung digestion evaluation)

The lung fiber burden was evaluated using two independent methods in the study. The first method, the results of which are presented in this section through 91 days post-exposure, was through the digestion of the entire lung without differentiating where in the lung the fibers are located with evaluation of fiber size distribution using scanning electron microscopy. The second method was using confocal microscopy which provided the localization of fibers in the lung compartment, including fiber burden and size.

Table 1
Aerosol concentration and size distribution of the exposure atmosphere in the air control group 1, chrysotile and brake dust group 2, brake dust group 3 and crocidolite asbestos group 4.

Exposure group	Gravimetric concentration mg/m ³ (SD)	Total Number of fibers counted on the filter*	Number of total fibers/cm ³	Percent WHO fibers/cm ³	Percent of fibers $\geq 20 \mu\text{m}/\text{cm}^3$	Percent of all fibers $\geq 20 \mu\text{m}/\text{cm}^3$	Mean number particles/cm ³	Diameter Range (μm)	Length range (μm)	GMD (Std. Dev.) (μm)	GML (Std. Dev.) (μm)	Mean diameter (μm) Std. Dev.	Length weighted arithm. diameter (μm)	Length weighted geom. diameter (μm)	Aspect ratio
(Group 1) Air Control	0	7	0.002	0.001	42.9	0	0	0.006	0.5	2.3	1.11	4.49	1.20	1.23	4.07
(Group 2) Chrysotile	3.48	2454	6953	1007	14.5	189	3140	0.03	0.03	0.6	1.53	1.46	0.20	0.16	29.8
(Group 3) Brake dust	1.52	1623	389.3	46.0	11.8	3.6	1240	0.05	0.05	0.6	0.21	2.25	0.32	0.24	16.99
(Group 4) Crocidolite	6.34	1820	2013	709	35.2	93	602	0.05	0.7	0.34	1.79	2.00	0.50	0.39	17.62
	0.42							–2.6	–190	1.64	2.44	0.21			

SD: Standard deviation; GMD: Geometric mean diameter; GML: Geometric mean length; MMAD: Mass median aerodynamic diameter.

* The total number of fibers counted on the filter is based upon the rules specified in section "Fiber/Particle Analysis and Lung Digestion" above.

** For the brake dust group 3, the MMAD = 1.89 (Geometric standard deviation = 2.54) as determined by the impactor measurement.

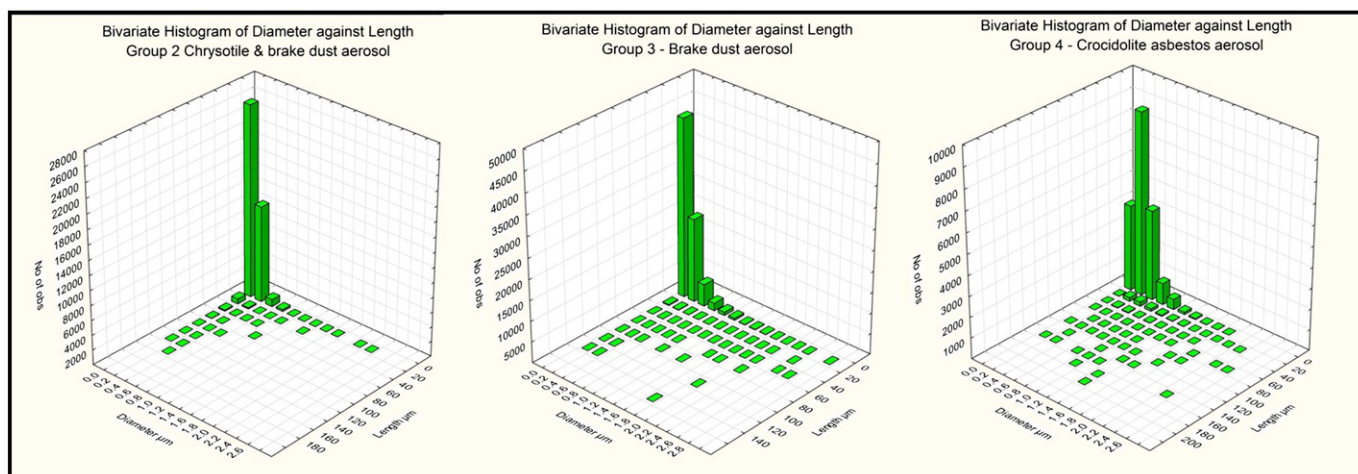


Fig. 3. Bivariate length and diameter distributions of the exposure aerosols in the chrysotile and brake dust group 2, brake dust group 3; and crocidolite asbestos group 4.

The mean concentrations and dimensions of the fibers as determined by lung digestion evaluation at each time point through 91 days post exposure for groups 2–4, respectively, are presented in the supplemental data in Tables S3–S5.

The lung burden immediately after cessation of the 5 days of exposure (day 0) is a product of the clearance dynamics of the fibers in the lung since the start of the 5 days of exposure. Immediately following the cessation of the last exposure there was a mean of 0.1 million fibers longer than 20 μm in the lung in the chrysotile and brake dust exposure group (2). In the brake dust group (3) there were 0.016 million fibers longer than 20 μm in the lung which corresponds to the lower exposure concentration of chrysotile in this group. In the crocidolite exposure group (4) there were 3.4 million fibers longer than 20 μm in the lung at day 0.

In the brake dust groups with or without added chrysotile the number of fibers greater than 20 μm in length diminishes rapidly after cessation of exposure. These fibers appear to break apart into shorter fibers with the number of fibers less than 5 μm increasing from a mean of 24 million on day 0 to 36 million on day 1 and 57 million on day 7. The number of fibers 5–20 μm in length also increased from 1.8 million on day 0 to 2.7 million on day 1. The bivariate length and diameter distribution of the fibers in the lung at days 0 and 91 are shown in Fig. 5 for the 3 exposure groups. In the chrysotile and brake dust group the

number of longer fibers are reduced as they are broken down into shorter fibers. The number of thin shorter fibers (<10 μm length) are increasing as a result. In the brake dust group the lung concentration immediately following cessation of exposure was correspondingly less with the shorter chrysotile fibers present also clearing.

By 91 days after cessation of exposure approximately 90% of the longer fibers have been cleared from the lung in group 2 with an average of only nine fibers detected on the filter in the SEM microscopic analysis. In group 3, between 1 and 5 fibers were detected at 91 days on the filter in the SEM microscopic analysis. The regional localization of fibers using confocal analysis as discussed below provides a basis for assessing that these few fibers observed are likely in the bronchial tree and not in the alveolar region of the lung. By 91 days, 95% of all fibers observed in the lung in the chrysotile and brake dust group were less than 5 μm in length. The geometric mean length of the fibers in the lung at 91 days was 2.3 μm. As the lung digestion procedure provides only a total estimate of the number of fibers in all the lung compartments without the ability to differentiate where in the lung each fiber is located, this procedure cannot address the question of where these fibers are in the lung.

In the crocidolite asbestos exposure group the fibers longer than 20 μm which are less than 1 μm in diameter (rat-respirable to the lung parenchyma), have approximately the same distribution pattern at 91 days as compared to 0 days. It is only the shorter thinner crocidolite fibers which show clearance. Due to the insolubility of the crocidolite fibers, the longer fibers do not disintegrate into shorter fibers as occurs in the chrysotile exposure groups.

As described above, the air control group was exposed to filtered air without any fibers using similar aerosol generation and exposure systems. The lungs from the control animals were processed and analyzed using the same procedures. A low level background of shorter chrysotile fibers was detected in some of the air control lungs samples on days 0 and 14 that were low-temperature ashed which was less than 0.001 of the exposed values. No fibers longer than 20 μm were found in any of the control sample. No crocidolite fibers were found in any of the control samples. The confocal microscopy measurements found no fibers in any of the air control lungs indicating that the background was due to the ashing procedure and not from inhalation exposure.

Fiber clearance (from the lung digestion evaluation)

The clearance half-times for each fiber range are shown in Table 2. The clearance curves for each fiber range are shown in Figs. S-7 through S-10. These were determined using the statistical procedures specified in the EC protocol (EUR, 18748 EN, 1999). The clearance curves were

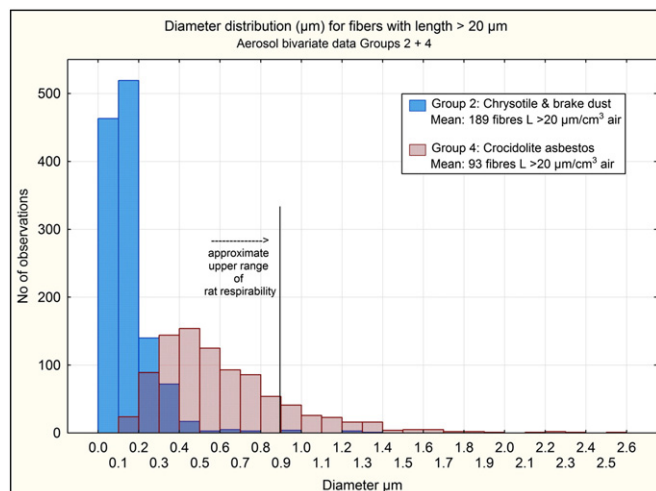


Fig. 4. Diameter distribution of the fibers longer than 20 μm in groups 2 and 4.

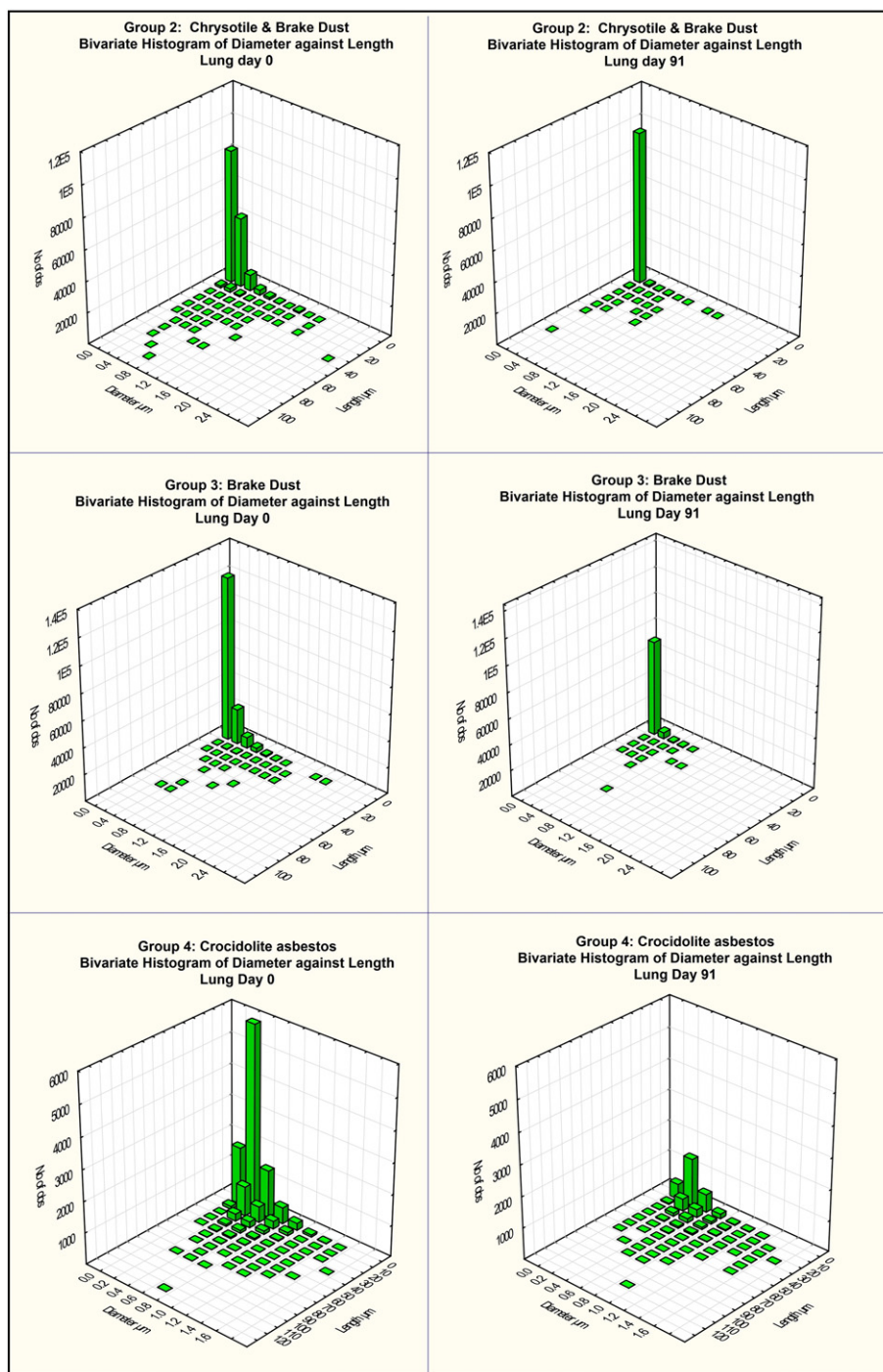


Fig. 5. Bivariate length and diameter distributions of fibers in the lung in the chrysotile and brake dust group 2; brake dust group 3; and crocidolite asbestos group 4 at 0 days and 91 days after cessation of exposure. (The No. obs. is number of fibers.)

fitted to the data using nonlinear regression techniques with a single or double exponential (StatSoft, Inc., 2011) and were based upon the initial results available through 91 days post exposure.

The clearance rate from the lung of the chrysotile fibers longer than 20 μm is similar in the chrysotile-brake dust group and the brake dust alone group with estimated half-times of 33 and 30 days.

The impact of the larger number of short fibers and relatively insoluble particles in the chrysotile and brake dust group is reflected in the estimated clearance half-times with of 52 days for the shorter fibers and 510 days for the particles. In contrast, the brake dust group

which had nearly 20 times fewer shorter fibers and 4 times fewer particles than the chrysotile-brake dust group, also had faster clearance half-times for the fibers less 5 μm in length of 45 days and of particles of 47 days.

In contrast, in the crocidolite asbestos group, following the clearance of the fibers longer than 20 μm which deposit in the tracheal-bronchial tree, those longer fibers remaining in the parenchyma persist in the lung with a clearance half-time estimated to be greater than 1000 days. Following cessation of exposure, the short crocidolite fibers begin to clear, however, by 32 days the clearance rate has diminished and plateaus

Table 2

Estimated Fiber Clearance Half Times in days (through 91 days post exposure) (SE: Standard error).

Group	Exposure	Fibers L>20µm (days)	Fibers 5–20µm	Fibers<5µm	Particles
2	Chrysotile & brake dust	33 (SE:11)	23 (SE: 12)	52 (SE: 42)	510 (SE: 1922)
3	Brake dust	30 (SE: 11)	41 (SE: 15)	45 (SE: 23)	47 (SE: 42)
4	Crocidolite asbestos*	> 1000	> 1000	> 1000	> 1000

* The standard errors for the crocidolite estimates could not be calculated due to the lack of clearance.

through 91 days. The clearance half time of the remaining shorter fibers and particles is estimated also to be greater than 1000 days.

Pathological findings in the lung

Histopathological examination

The fiber clearance results clearly differentiate chrysotile fiber retention in both the chrysotile-brake dust group and the brake dust alone group from that of crocidolite asbestos; the histopathology findings provide a basis for determining the biological relevance of this difference.

The summary of histopathological findings in the lung through 91 days after cessation of exposure is presented in Table S-6 (supplemental data) which shows the specific histological findings seen in the lung and the mean grade observed for each finding. Severity was scored on the following scale: no lesions, minimal, slight, moderate, marked, or massive (grades 0–5 respectively). A summary of the key lung histopathology scores through 91 days post exposure is presented in Fig. 6.

There were no exposure-related histopathological findings in animals exposed to filtered air. In the chrysotile-brake dust group and brake dust alone group, slight accumulation of particle laden macrophages were observed from 7 through 91 days post exposure. At 32 days post exposure, very slight (multi)focal particle laden microgranulomas at the bronchiole–alveolar junctions were observed in groups 2 and 3, however, there were no associated giant cells. These findings are illustrated at 0 and 91 days in micrographs in Fig. 7.

In the crocidolite asbestos exposure group, accumulation of fiber laden macrophages was observed already at day 0, immediately after cessation of exposure. This increased at day 7 and was associated with the formation of (multi)focal fiber laden microgranulomas at the bronchiolo–alveolar junctions with multinucleate (syncytial) giant cells within these microgranulomas. By day 32, interstitial fibrosis was

observed. These findings persisted through 91 days post exposure (Fig. 7). The concurrent development of the fibrosis is illustrated in the micrographs stained with Masson's tri-chrome at 91 days post exposure (Fig. 8, panel D). Masson's tri-chrome is specific to collagen which is shown as blue in the images. Panels A, B, and C of Fig. 8 show the air control brake dust with chrysotile and brake dust alone groups, all of which are similar in appearance. The development of the fibrotic lesions in the crocidolite asbestos exposure group is also reflected in the interstitial fibrosis score (Fig. 6). No fibrosis was observed in the other groups.

The lungs were also evaluated by the pathologist for the Wagner score (McConnell et al., 1984; McConnell and Davis, 2002). The Wagner score specified that “the grading system made a clear differentiation (break) between Grade 3 and Grades 4–8, with the former representing “cellular change” (inflammatory and reversible) and the latter progressive degrees of fibrosis (not totally reversible)”.

The Wagner score for both the chrysotile and brake dust group and the brake dust alone group ranged between 1 at day 0 and up to 2 through 91 days post exposure, where 1 is no lesion observed and 2 is a few macrophages in the lumen of the terminal bronchioles and alveoli. With the crocidolite asbestos exposed animals, the Wagner score started at 2 on day 0 and increased up to 4 through 91 days post exposure (Grade 4: Minimal collagen deposition at the level of the terminal bronchiole and alveolus. Increased bronchiolization with associated mucoid debris suggesting glandular pattern.)

Pulmonary fibrosis analysis – confocal microscopy

The connective tissue (elastin and collagen) present in the lung was measured by confocal microscopy to obtain the percentage of the elastin and collagen per area of lung tissue (%CT/FOV). For each group and time point 300 cubic lung tissue volumes of $112,550 \mu\text{m}^3$ each were imaged, the amount of connective tissue measured and the number and length of the fibers observed were recorded. Fields of view that contained a blood-vessel of diameter greater than $50 \mu\text{m}$ were not included due to the high amount of collagen in the blood-vessel walls.

The percent fibrosis is shown in Fig. 9 for each group at 0, 32 and 91 days after cessation of the 5 day exposure. In the air control group the percent connective tissue ranged from a mean of 3.8 ± 2.9 at day 0; 6.4 ± 4.4 at day 32 and 2.9 ± 2.2 at day 91 with a range in individual values over this period of 0.2 to 27%. Compared to the air control group, there were no statistically significant trends in the chrysotile & brake dust group or in the brake dust group alone with or without fibers present. The chrysotile fibers present in the tissues had no impact on the development of connective tissue and did not cause a fibrotic response through 91 days post exposure.

In the crocidolite asbestos exposure group, there is a consistent statistically significant increase in the mean amount of connective tissue present compared to day 0 (mean 4.4 ± 3.4) with means of 8.0 ± 4.4 at 32 days and 14.7 ± 12.8 at 91 days post exposure compared to day zero as determined by analysis of variance (Table S-5, supplemental data). At 91 days, when compared to the air control group the mean connective tissue in the crocidolite asbestos exposure group increased by 5 times. The range of individual measurements shows that at day 0 the percent connective tissue in the crocidolite asbestos exposure group was similar to that found in the air control, however, by 91 days

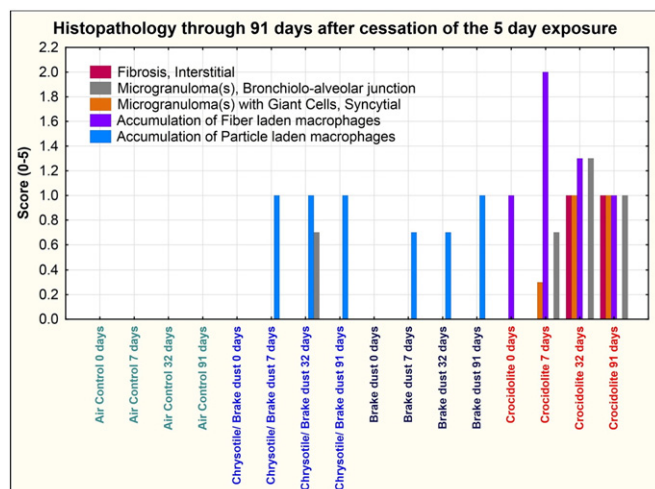


Fig. 6. Summary of lung histopathology scores through 91 days post exposure.

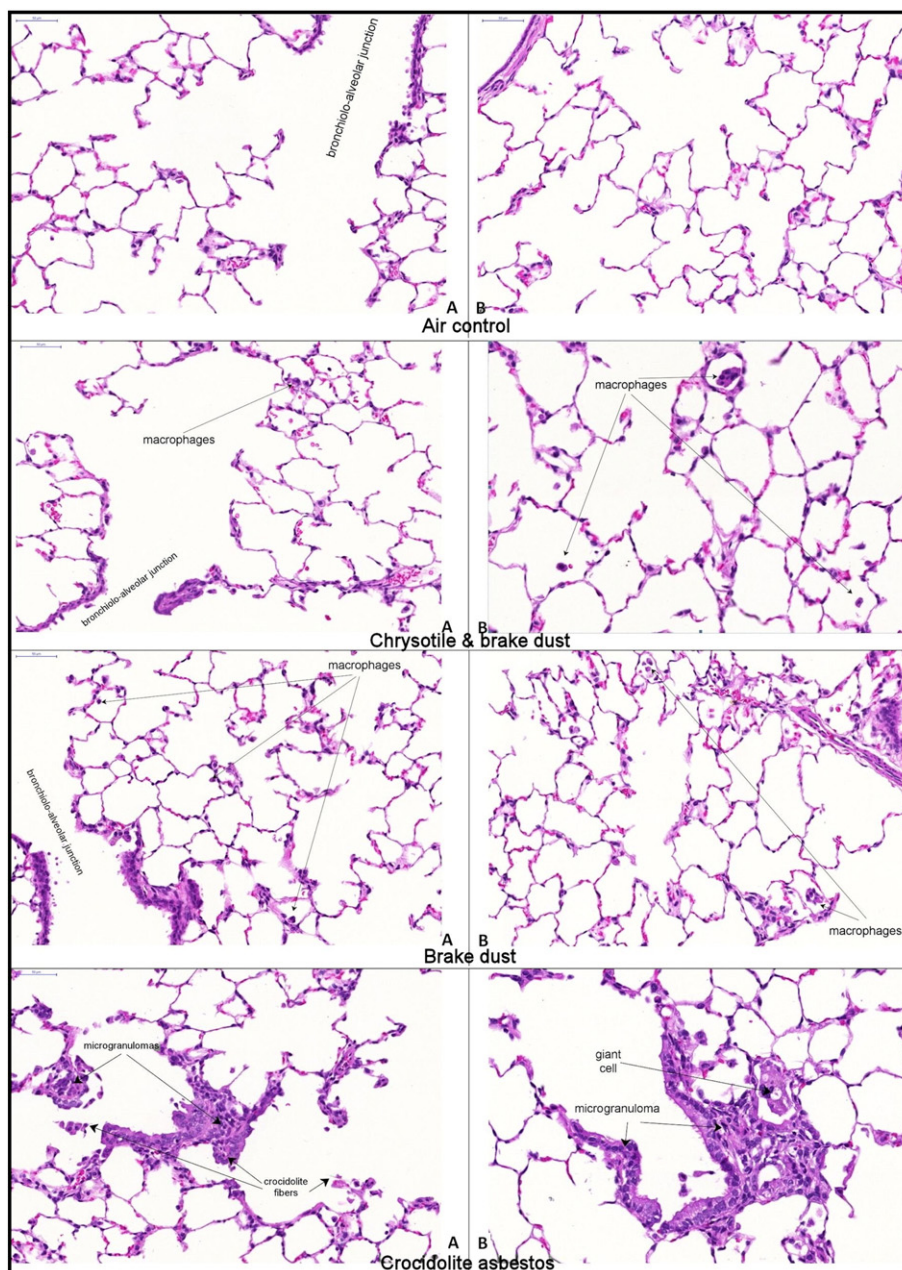


Fig. 7. Histopathological photomicrographs of groups 1–4 at 0 and 91 days post exposure: Group 1 Air control: A: day 0 showing bronchiole-alveolar junction and adjacent alveoli (400 \times). B: 91 days showing alveoli (400 \times). Group 2 Brake dust & chrysotile: A: 0 days showing bronchiole-alveolar junction and adjacent alveoli with a few macrophages (400 \times). B: 91 days showing alveoli with a few macrophages (530 \times). Group 3 Brake dust: A: 0 days showing bronchiole-alveolar junction and adjacent alveoli with a few macrophages (400 \times). B: 91 days showing alveoli with a few macrophages (530 \times). Group 4 Crocidolite asbestos: A: 0 days showing inflammatory response with microgranulomas. Crocidolite fibers are also observed (400 \times). B: 91 days showing alveoli filled with inflammatory cells forming microgranulomas with giant cell (530 \times).

post exposure, the connective tissue range in group 4 increased in fields of view to up to 87%.

The confocal microscopy images (Figs. 10 and 11) show the comparative connective tissue response. The connective tissue is imaged as the bright white structures. The parenchyma immediately after cessation of exposure (day 0) is shown in Fig. 10. A normal interstitial wall of the lung lined with a thin layer of collagen is seen in the air control group 1 with occasional alveolar macrophages in the alveolus. In the chrysotile and brake dust group 2 and the brake dust alone group 3 similar patterns of collagen are also observed with a few additional macrophages that responded to clear the inhaled dust (shown in red). In the crocidolite asbestos group 4, an alveolus is seen filled with inflammatory cells and interlaced with a collagen matrix. A long

crocidolite fiber is seen in the adjacent alveolus surrounded by a few macrophages.

By 91 days post exposure, the air control, chrysotile/brake dust and brake dust groups (1, 2 and 3) are very similar in appearance with a few macrophages observed on the distal ciliated airway (Fig. 11). In the crocidolite asbestos group 4, a collagen-interlaced hyperplasia marked by interstitial fibrosis is observed in the region of the alveolar duct (panel a). The intensive collagen matrix obscures the normal structure and is associated with crocidolite fibers intertwined within the matrix. Only the ends of the fibers are seen as this is a 2 dimensional image. In panel (b) long crocidolite fibers are observed in a terminal bronchial hyperplasia which is interlaced with a dense collagen matrix.

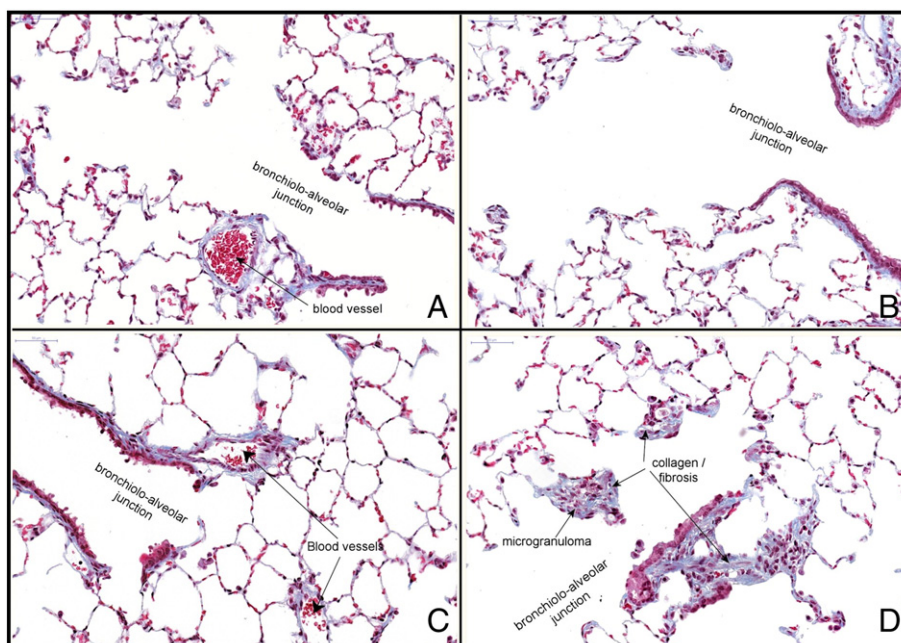


Fig. 8. Histopathological photomicrographs with Masson's trichrome stain at 91 days (400 \times). Panels A, B, & C: Group 1 Air control, group 2 Chrysotile and brake dust and group 3 Brake dust are all similar in appearance. In groups 1 and 3, blood vessel(s) can also be seen. Panel D: Group 4 Crocidolite asbestos. The Masson's trichrome stain shows inflammatory response with microgranuloma with extensive collagen and fibrosis (blue color).

Regional quantification of fibers in the lung

Airway versus parenchyma. An issue that is often of concern with inhalation toxicology studies is to assure that the test material being evaluated has reached the site in the lung where disease can develop. The confocal

microscopy procedures used in the study provide the ability to determine not only the fiber size distribution in the lung but where within the lung compartments these fibers are located.

The number of fibers deposited in the airways and parenchyma was estimated through the confocal microscopy fiber measurements. The

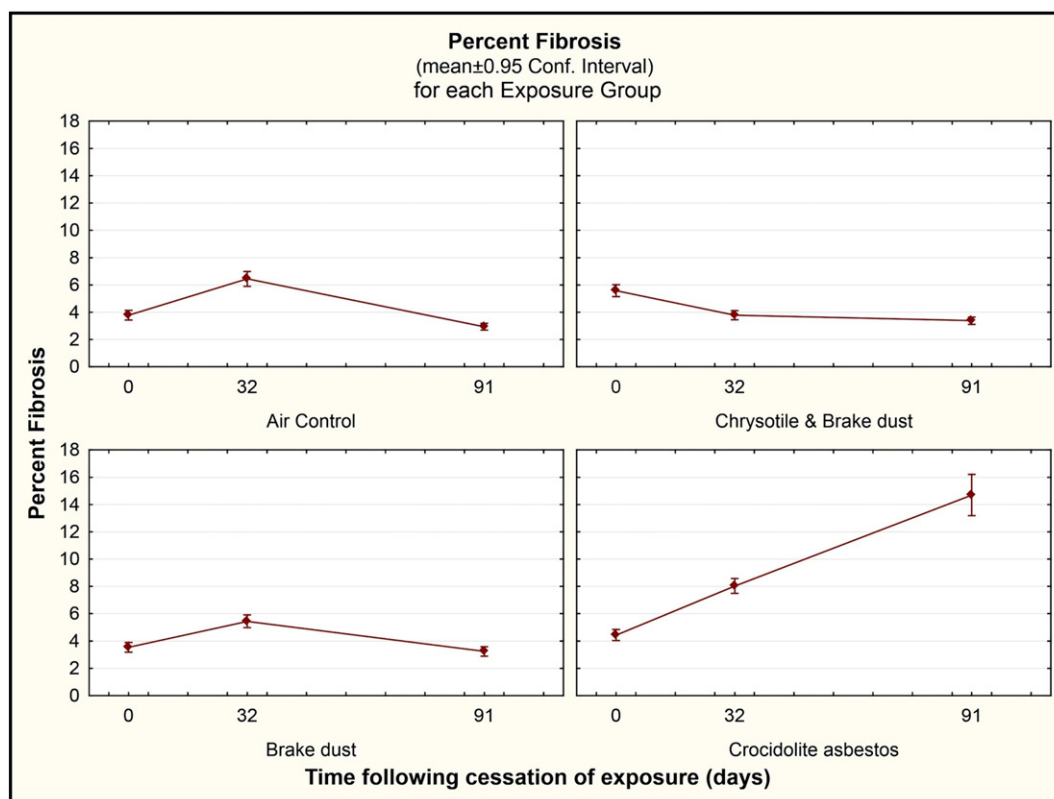


Fig. 9. Confocal microscopy: Percent connective tissue in the lung per field of view (Animal means \pm 0.95 Conf. Interval) for groups 1 Air control, 2 Chrysotile & brake dust, 3 Brake dust and 4 Crocidolite asbestos. For crocidolite asbestos, the correlation coefficient is $r = 0.83$, $p = 0.0055$.

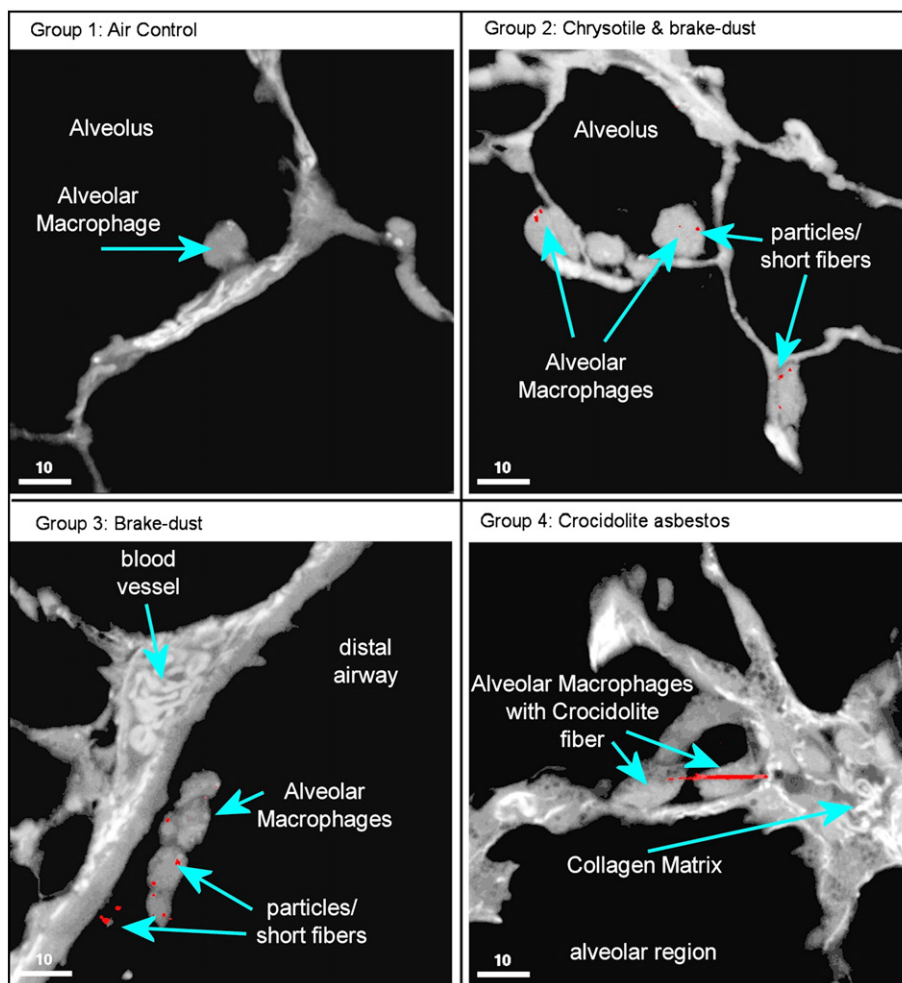


Fig. 10. Confocal microscopy Interstitial Fibrosis Assay — day 0: Group 1 Air control: A normal interstitial wall of the lung lined with a thin layer of collagen is seen in the air control group 1 with occasional alveolar macrophages in the alveolus. Group 2 Chrysotile & brake dust: A few macrophages are observed in the alveoli. Chrysotile or brake dust particles can be observed within the macrophages. Group 3 Brake dust: A few macrophages are observed in the distal airway. Chrysotile or brake dust particles can be observed within the macrophages. A blood vessel is also seen. Group 4 Crocidolite asbestos: An alveolus is seen filled with inflammatory cells and interlaced with collagen (fibrosis) shown in white. A long crocidolite fiber (~20 µm) is observed in an adjacent alveolus with macrophages at each end.

number of fibers in the total lung volume was estimated based upon the regions sampled in the lung by confocal microscopy. These values should be viewed as estimates as they are influenced by the orientation of fibers within the lungs and the degree of inflation of the lungs. As presented above the clearance rates as determined by confocal correlate with those determined by the lung digestion procedure. In each of the three exposure groups, more than 99% of the fibers were observed in the parenchyma immediately after cessation of exposure.

Fiber clearance by length fraction in the airways versus the parenchyma. The fiber clearance by length fraction was also estimated from the 3D confocal images in the airways and parenchyma. Table 3 shows for each exposure group the percent of the total number of fibers observed at day 0 in the parenchyma and in the airways for the length fractions <5 µm, 5–20 µm and >20 µm at 0, 7, 32 and 91 days post exposure.

For both the chrysotile and brake dust group and the brake dust alone group, nearly all of the fibers longer than 20 µm were observed in the parenchyma. In both of these groups, by 91 days post exposure the chrysotile fibers were no longer observed. In the airways, chrysotile fibers longer than 20 µm were only observed at 91 days post exposure in the brake dust group.

In the crocidolite asbestos exposure group 15% of the fibers in the airways and 14% of the fibers in the parenchyma were longer than 20 µm immediately after cessation of exposure. As also observed in the lung digestion procedure, these longer crocidolite fibers persisted and accounted for 9% (parenchyma) and 7% (airways) of the fiber present at 91 days post exposure.

Localization of fibers within the airways and parenchyma

The location of fibers within the following lung compartments was also determined by confocal microscopy using random search procedures as shown below.

Airway region, if the fiber was:

- Penetrating the airway wall or located completely underneath the airway wall. Partly or fully embedded into the interstitial space, blood vessel, or lymphatics.
- In airway lumen; portion of fiber visualized not touching tissue.
- Wholly or partly inside airway macrophages.
- On surface of or intercalated within ciliated epithelium of conducting airway

Parenchyma region, if a fiber was:

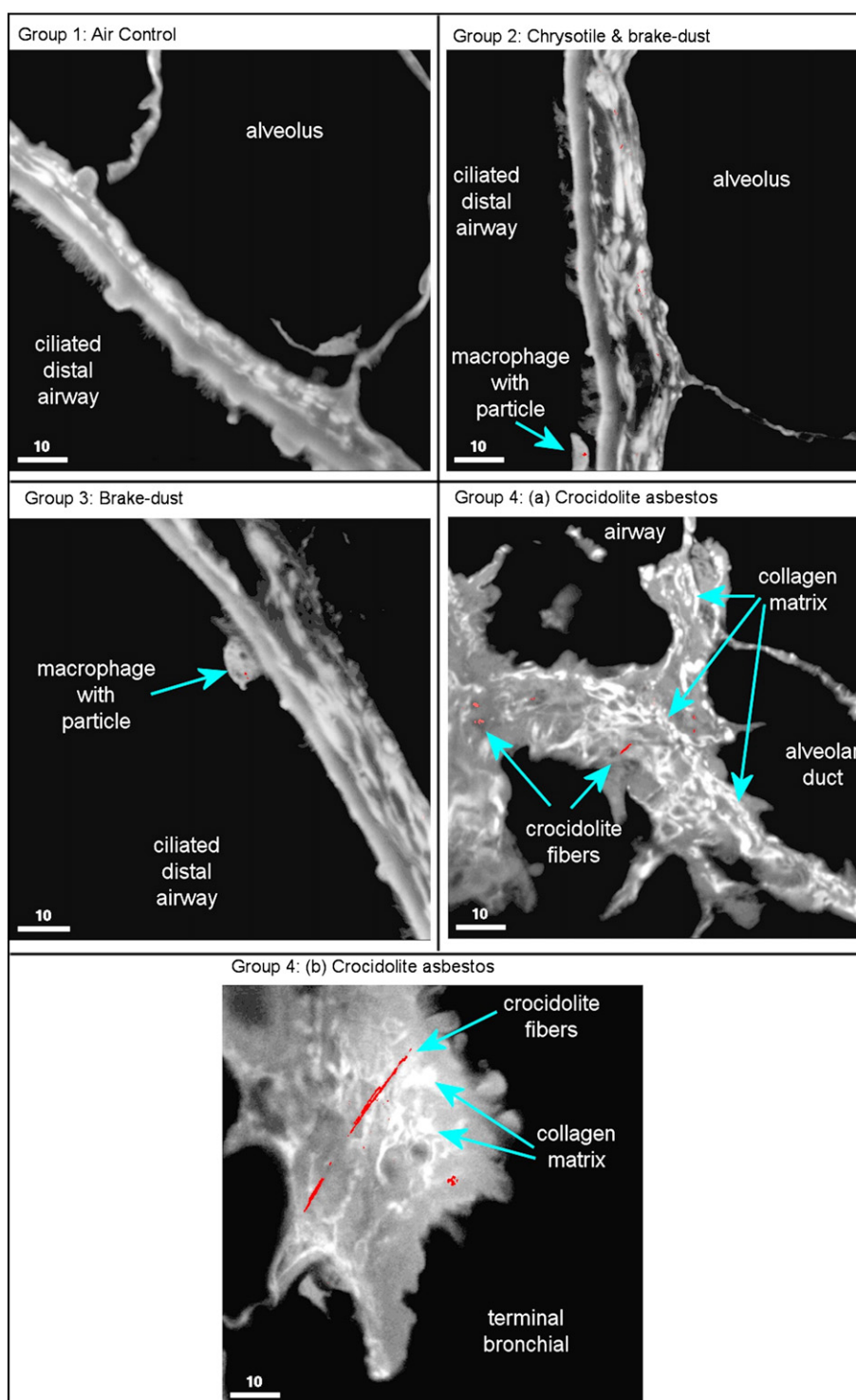


Fig. 11. Confocal microscopy Interstitial Fibrosis Assay — 91 days: Group 1 Air control shows a typical profile of ciliated airway epithelium. Group 2 Chrysotile & brake dust: A few macrophages are observed on the ciliated distal airway. A few chrysotile or brake dust particles can be observed within the macrophages. Group 3 Brake dust: A macrophage is observed on the ciliated distal airway. Chrysotile or brake dust particles can be observed within the macrophage. Group 4 Crocidolite asbestos: Intense inflammatory response interlaced with collagen (white) to the crocidolite fibers in the region adjacent to the airway and alveolar duct.

- Partly or intercalated within the interstitial space, blood vessel, or lymphatic vessel.
- Observed in alveolar ducts but not in contact with tissue.
- Wholly or partly inside alveolar macrophages.
- In contact with epithelium, alveoli, alveolar ducts, or terminal bronchioles.

The distribution of fibers in each group within the airway and the parenchyma are shown in Figs. 12 and 13, respectively.

In the chrysotile and brake dust exposure group, immediately following cessation of exposure a mean of 260,000 (SD²: 97,000) fibers

² SD: Standard deviation.

Table 3
Confocal microscopy analysis: Percentage of total fibers at day 0 observed in the parenchyma and the airways by the random analysis with confocal microscopy for groups 1 Air control, 2 Chrysotile & brake dust, 3 Brake dust and 4 Crocidolite asbestos as a function of time through 91 days.

Group	Day	Parenchyma %				Airways %			
		All parenchyma fibers	Fibers Length <5 μ m	Fibers Length 5–20 μ m	Fibers Length >20 μ m	All Airway Fibers	Fibers Length <5 μ m	Fibers Length 5–20 μ m	Fibers Length >20 μ m
Chrysotile & Brake dust	0	100%	76.5	22.6	0.9	100%	64.86	35.14	0.00
Chrysotile & Brake dust	7	25	19.6	5.2	0.3	25	16.22	18.92	0.00
Chrysotile & Brake dust	32	37	33.6	3.4	0.3	37	5.41	0.00	0.00
Chrysotile & Brake dust	91	1.5	1.5	0.0	0.0	1.5	0.00	5.41	0.00
Brake dust	0	100%	24.3	64.9	10.8	100%	36	64	0
Brake dust	7	105	59.5	45.9	0.0	4	0	4	0
Brake dust	32	27	13.5	10.8	2.7	12	4	8	0
Brake dust	91	11	8.1	2.7	0.0	8	4	0	4
Crocidolite	0	100%	25	61	14	100%	28	58	15
Crocidolite	7	91	22	58	10	77	30	41	6
Crocidolite	32	73	26	36	11	24	3	17	4
Crocidolite	91	31	3	20	9	26	2	17	7

longer than 5 μ m were observed in the airways with the majority located either within airway macrophages or on the airway lumen (Fig. 12). By 91 days, the majority of fibers in the airways had cleared with the remaining fibers observed on the ciliated epithelium which suggests that these fibers were in the process of being cleared as well.

In the parenchyma, in the chrysotile-brake dust group more than 300 million (SD: 99 million) fibers were estimated to be in the parenchyma immediately after cessation of exposure (Fig. 13). The majority of these fibers were either in airway macrophages or in contact with epithelium, alveoli, alveolar ducts, or terminal bronchioles suggesting that they were actively involved in being cleared from the lung. By 91 days, 97% of the fibers had been cleared with those remaining found either in airway macrophages or in contact with epithelium, alveoli, alveolar ducts, or terminal bronchioles.

In the brake dust group, immediately following cessation of exposure a mean of approximately 170,000 (SD: 115,000) fibers longer than 5 μ m were observed in the airways corresponding to the lower fiber exposure in this group. The majority of fibers were located either within airway macrophages or on the airway lumen (Fig. 12). By 91 days, most of the fibers in the airways had cleared with the remaining fibers observed on the airway lumen.

In the parenchyma, in the brake dust group approximately 40 million (SD: 38 million) fibers were observed in the parenchyma immediately after cessation of exposure (Fig. 13). The majority of these fibers were either in airway macrophages or in contact with epithelium, alveoli, alveolar ducts, or terminal bronchioles. By 91 days, approximately 90% of the fibers had been cleared with those remaining found either in airway macrophages, alveolar ducts or in contact with epithelium, alveoli, alveolar ducts, or terminal bronchioles.

In the crocidolite asbestos exposure group a different pattern was observed. After cessation of exposure, more than 2 million (SD: 0.5 million) crocidolite fibers were estimated to be in the airways located wholly or partly inside airway macrophages, on the surface or intercalated within ciliated epithelium of the conducting airway, in airway lumen and also penetrating the airway wall or located completely underneath the airway wall, partly embedded in the interstitial space, blood vessel or lymphatics (Fig. 13). By 91 days, while more than 80% of the fiber had cleared, 350,000 (SD: 150,000) crocidolite fibers were estimated to remain in the airways largely either in airway macrophages or on the surface or intercalated within the ciliated epithelium of the conducting airways.

In the parenchyma at day 0, more than 200 million (SD: 19 million) crocidolite fibers were estimated to be either in alveolar

macrophages or in contact with epithelium, alveoli, alveolar ducts or terminal bronchioles. At 32 days, while the majority of fibers were still found in alveolar macrophages or in contact with epithelium, alveoli, alveolar ducts or terminal bronchioles, a significant portion of fibers were now observed partly or intercalated within the interstitial space, blood vessels or lymphatic vessels. By 91 days, there were approximately 86 million (SD: 20 million) crocidolite fibers remaining in the parenchyma with most in similar compartments as at 32 days post-exposure. As presented in Table 3, approximately 1/3 of the observed fibers in the parenchyma at 91 days post exposure were longer than 20 μ m.

Discussion

This study was designed to determine the persistence, translocation and pathological response of the lung and pleural cavity to dust emitted from grinding of drum brakes that incorporated chrysotile into the matrix. This is the first study to evaluate brake dust by inhalation in an animal model. The interim results presented here on the lung provide a basis for evaluating the biopersistence and pulmonary response of both brake dust alone and brake dust combined with added chrysotile in comparison to the amphibole crocidolite asbestos following short term exposure. The results through 365 days including pleural translocation and response will be presented in a subsequent paper.

This study has evaluated the exposure to the full brake dust matrix and the combined exposure of the brake dust with added chrysotile. This study has not examined the possible effect of any co-exposures which may occur in parallel with brake dust exposure. The choice of exposure groups and concentrations was based upon the European Commission (EC) and the US Environmental Protection Agency (USEPA) (EUR, 18748 EN, 1999; ILSI, 2005) recommendations of having at least 100 fibers with length >20 μ m/cm³ in the exposure atmosphere. Given this requirement, we included group 2 as a mixed brake dust and added chrysotile exposure to address the 'worst case' scenario of the relatively insoluble particles from brake dust matrix interacting in the lung to produce an added or synergistic effect with the clearance of the chrysotile and the potential for pathological response. Group 3, brake dust, was included to provide a comparative group of exposure to the brake dust matrix alone, in order to evaluate particle effect from this matrix.

Crocidolite asbestos was included as a positive control to provide comparison to an amphibole asbestos. The crocidolite asbestos sample used in the study was unique as it was obtained as a commercial crocidolite asbestos sample (from Voorspoed mine, South Africa) which facilitated aerosol generation of the recommended exposure concentration

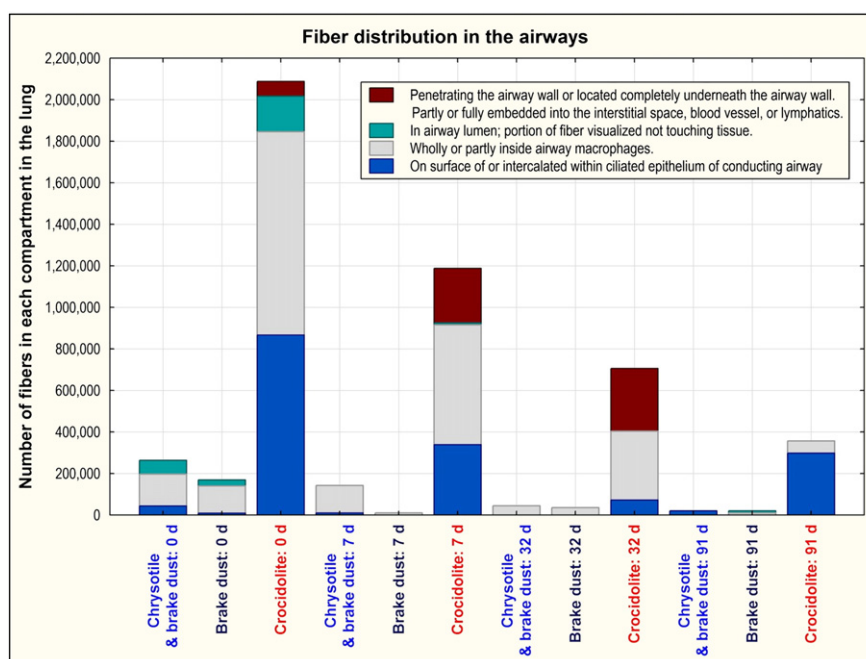


Fig. 12. Confocal microscopy: Compartmental fiber distribution in the airways for groups 1 Air control, 2 Chrysotile & brake dust, 3 Brake dust and 4 Crocidolite asbestos as a function of time through 91 days.

of fibers longer than 20 μm . The exposure concentration was chosen to meet the USEPA and EC recommendations.

The findings of the study are consistent with the current understanding of the differences in mineralogy and biopersistence of chrysotile fibers in brake dust compared to amphibole asbestos. Chrysotile is an acid soluble (Kobell, 1834) sheet silicate and is formed with rolled or concentric thin sheets (7.3 Å thick) composed of silicate and brucite layers with the magnesium hydroxide part of each layer closest to the fiber surface (Whittaker, 1963, 1957; Tanji et al., 1984; Titulaer et al., 1993). The magnesium is readily attacked by acid milieu such as occurs inside the

macrophage (pH 4–4.5), and dissociates from the crystalline structure, leaving an unstable silicate sheet. This process causes the thin rolled sheet of the chrysotile fiber to break apart and decompose into smaller pieces. These pieces can then be readily cleared from the lung by macrophages through mucociliary and lymphatic clearance.

In contrast, crocidolite asbestos is formed as solid rods/fibrils with the silica on the outside of the fibrils which makes it very strong and durable (Skinner et al., 1988; Whittaker, 1960). Due to the structural matrix of amphibole fibers, they are formed as solid fibrils and lack acid-soluble surface groups, resulting in negligible solubility at any pH

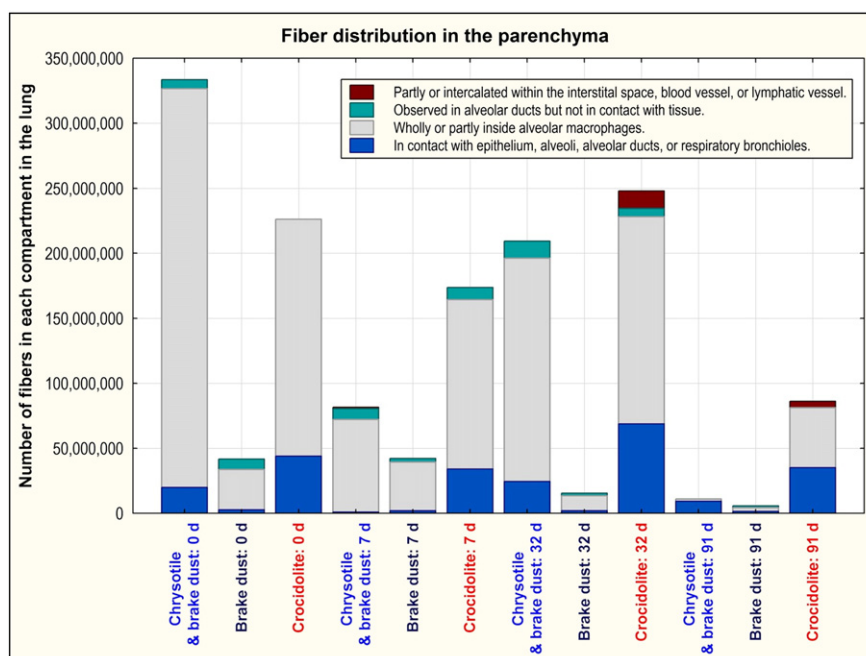


Fig. 13. Confocal microscopy: Compartmental fiber distribution in the parenchyma for groups 1 Air control, 2 Chrysotile & brake dust, 3 Brake dust and 4 Crocidolite asbestos as a function of time through 91 days.

Table 4

Fiber concentration and diameter and length range of the aerosol in the current study and Bernstein et al. (2010).

Study	Fiber grade	Number of total fibers/cm ³	Number WHO fibers/cm ³	Number of fibers ≥20 μm/cm ³	Diameter range (μm)	Length range (μm)
Chrysotile & brake dust (current study)	Added chrysotile 5R04	6953	1007	189	0.03–2.4	0.6–160
Brake dust (current study)	Section 3.3	389.3	46.0	3.6	0.05–2.9	0.6–140
Chrysotile & sanded material (Bernstein et al., 2010)	Added chrysotile 7RF3	6543	1496	295	0.01–0.6	1.0–180

that might be encountered in an organism (Speil and Leineweber, 1969).

One of the key factors in evaluating inhalation biopersistence/toxicology studies is accessing the respirability of the fibers (rat respirable: <~1 μm, Morgan, 1995; Weir and Meraz, 2001) and the resulting comparative exposure. In the chrysotile and brake dust aerosol 99% of the fibers $L > 20$ μm were <1 μm in diameter (rat-respirable) with 95% <0.4 μm in diameter. In the brake dust group, 90% were <1 μm in diameter (rat respirable) with 63% of the fibers <0.4 μm in diameter. In the crocidolite asbestos group, 88% of the long fibers were <1 μm in diameter (rat-respirable) with 21% <0.4 μm in diameter (Fig. 4). Thus fibers in all groups were largely respirable in the rat with chrysotile fibers in group 2 having the highest percentage of thinner fibers.

While the samples in this study were prepared in a similar fashion as those in Bernstein et al. (2010), Table 4 shows that the range of fibers diameters was greater in the 5R04 grade chrysotile in the current study compared to the grade 7RF3 chrysotile used in the earlier study. While in Bernstein et al. (2010) the largest diameter fiber was 0.6 μm, in the current study fibers up to 2.9 μm were in the aerosol. These larger diameter fibers as observed by SEM were either bundles of fibrils or fibers with attached brake dust particles and were of diameters that would not be rat respirable to the lung parenchyma (<~1 μm, Morgan, 1995; Weir and Meraz, 2001).

The estimated clearance times of the fibers from the lung >20 μm were 32 days for the chrysotile and brake dust group and 30 days for the brake dust alone group. In comparison to the crocidolite asbestos exposure group which had an estimated clearance half-time >1000 days, the longer chrysotile fibers cleared rapidly. As a result of their geological formation, chrysotile can vary in characteristic depending upon the mine and processing of the ore. In earlier studies of chrysotile alone or of chrysotile mixed with a joint compound (Bernstein et al., 2003, 2004, 2005a, 2005b, 2008, 2011) the clearance half-time of the longer fibers ranged from 0.7 to 11.4 days. The lack of a fiber related response in the histopathological findings strongly suggests that the few (group 2: 6.5–10 fibers counted on the filter; group 3: 1–5 fibers counted on the filter) remaining fibers longer than 20 μm in the current study were in the airways and not in the parenchyma.

Of the fibers that were >1 μm in diameter on day 0 in the group 2 lungs, 46% were longer than 20 μm and ranged in length up to 71.5 μm. In group 3 lungs on day 0, 11% of the fibers >1 μm in diameter were longer than 20 μm and ranged in length up to 51 μm. Such fibers could become trapped in the lower airways and with the whole lung digestion procedure could not be differentiated in terms of location in the lung. The few longer fibers observed by confocal microscopy were observed in the airways. The clearance half-time of fibers longer than 20 μm that were less than 1 μm in diameter was 1.6 days for the chrysotile and brake dust group which is within the range of the earlier studies.

Another factor which differentiates this study from an earlier comparative product study of a chrysotile with and without joint compound (Bernstein et al., 2008) is the nature of the particulate matter in the product. With the joint compound, the particles were composed primarily of calcium carbonate and easily dissolved in the lung. The effect reported by Bernstein et al. (2008) for these particles was to stimulate the sequestering of macrophage. These particles did not accumulate and were not observed by either histopathology or confocal microscopy.

The matrix required for the brakes is composed of heat resistant materials designed for endurance (resistance to wear and severe use) such as epoxies and other strong binders which because of the product application could not be readily soluble (Bosch, 2011). In addition, to assure respirability in the rat, the brake dust was micronized in an in-line jet mill reducing the average diameter of the particles from that which occurs through the grinding process. With a MMAD of 1.9 μm in the brake dust group, density of approximately 2 g/cm³ (Blau, 2001) and brake dust exposure concentration of 1.5 mg/m³, there would have been approximately 10¹⁴ brake dust/cm³ in the brake dust exposure aerosol (assuming spherical particles). In the combined chrysotile and brake dust exposure group, the total would increase to ~10¹⁹ particles-fibers/cm³. Following exposure these particles were observed in macrophages in the lung. The particle clearance half-time for group 2 of 510 days suggests that this combined exposure concentration together with the high rate of decomposition into shorter fibers of the longer chrysotile fibers which adds to this fiber pool exceeded the ability of the lung to effectively clear the particles. High concentrations of insoluble nuisance dusts can result in lung overload which compromises the clearance mechanisms of the lung though reduced macrophage function and clearance, and even result in inflammation and a tumorigenic response in the rat (Bolton et al., 1983; Muhle et al., 1988; Morrow, 1988, 1992; Oberdörster, 1995).

The durability of longer chrysotile fibers compared to amphibole fibers has been investigated in-vitro by Osmond-McLeod et al. (2011). The durability of a number of fibers including long fiber amosite and long fiber chrysotile in a Gambles solution was assessed. The pH of the Gambles solution was adjusted to 4.5 to mimic that inside the macrophage phagolysosomes which the authors described as “potentially the most degradative environment that a particle should encounter following lung deposition and macrophage uptake”. The authors reported that the data indicate that long fiber chrysotile showed 70% mass loss and a marked decrease in length with long-term incubation in the Gambles solution, with a concomitant mitigation of the pathogenicity seen in mice injected with samples. In contrast, the amphibole asbestos amosite showed no fiber shortening and did not lose its pathogenicity. This and other studies assessing the difference between the serpentine mineral chrysotile and amphibole mineral crocidolite asbestos have been reviewed recently by Bernstein et al. (2013).

In contrast, to the chrysotile fibers the long crocidolite asbestos had an estimated clearance half time of >1000 days. In previous biopersistence studies with amphibole asbestos, the clearance half-time was reported to range from 418 to >1000 days (Musselman et al., 1994; Hesterberg et al., 1996, 1998; Bernstein et al., 2005b, 2011).

No significant pathological response was observed at any time point in response to the added chrysotile or the brake dust. A low level macrophage response was observed in response to the large number of particles in the exposure atmosphere, with no further evolution observed. The absence of pathological response in chrysotile/brake dust and brake dust groups was confirmed through classical histopathological examination which determined that the Wagner score ranged between 1 (unexposed normal-air control) and 2 (minimal cellular change). Quantitative fibrotic response was also evaluated through confocal microscopy which determined that the amount of connective tissue/fibrosis present following exposure in the chrysotile/brake dust

and brake dust groups was similar to that measured in the air control group.

Following 5 days of exposure to crocidolite asbestos, a notable inflammatory response occurred immediately following cessation of exposure with numerous long fibers observed in both the airways, distal airways and the parenchyma and associated with a cellular/macrophage response with collagen formation. The crocidolite fibers in the parenchyma and in the distal airways persisted with the inflammatory response progressing to Wagner grade 4 interstitial fibrosis within 32 days. The confocal assessment of the collagen in the connective tissue revealed a progression in connective tissue proliferation which increased linearly through 91 days ($r = 0.83$, $p = 0.0055$) with a 5-fold increase in mean collagen levels in the crocidolite group at 91 days, compared to the air control group.

As the exposure concentration for fibers longer than 20 μm in groups 2 and 4 were in the same range, if both fibers were equally biopersistent, the mean concentration of fibers longer than 20 μm in the lung would have been similar. As presented above, the fibers longer than 20 μm in the group 2 exposure aerosol were thinner than those in the group 4 aerosol with 98% less than 1 μm in diameter. This would suggest that the large majority of the longer chrysotile fibers would have deposited in the lung parenchyma and had cleared quickly with only the fibers in bundles which were most likely in the airways clearing more slowly. The clearance half-time of the long chrysotile fibers that were less than 1 μm in diameter was 1.6 days.

The results from this study provide a scientific basis that following short term exposure the no observable effect level for chrysotile in brake dust is less than 1000 WHO fibers/ cm^3 (including 189 fibers $L > 20 \mu\text{m}/\text{cm}^3$). In addition, these results support the lung burden and epidemiological studies reviewed by Marsh et al. (2011), Paustenbach et al. (2004), Laden et al. (2004), and Butnor et al. (2003), which differentiate that the chrysotile in brake dust is not associated with disease. These studies have taken into consideration possible confounders such as smoking and occupational exposures.

The pathological response following short term crocidolite asbestos exposure at a concentration of 709 WHO fibers/ cm^3 (including 93 fibers $L > 20 \mu\text{m}/\text{cm}^3$) emphasizes the importance of even small exposures to amphibole asbestos such as crocidolite in the etiology of asbestos related disease.

Conclusions

The interim results of this study show that there is an important difference in biopersistence and pathological response in the lung between brake dust derived from brake pads manufactured with chrysotile in comparison to the amphibole, crocidolite asbestos. The pathological response was determined using two independent methods. Classical histopathological examination was performed on thin lung sections with scoring of the collagen level at the bronchoalveolar junctions as well as the Wagner score. In addition, the collagen deposition in the connective tissue of the lung was evaluated using confocal microscopy in order to assess the fibrotic response.

No significant pathological response was observed at any time point in the brake dust or chrysotile/brake dust exposure groups. Slight macrophage accumulation was noted in response to the high particle exposure levels in the test atmospheres and the decomposition of the longer chrysotile fibers into shorter fibers or particles. This was reflected as well in the Wagner score which ranged from 1 to 2 (with one being the level in the air control group). The long chrysotile fibers cleared quickly with clearance halftimes estimated as 30 and 33 days respectively in the brake dust and the chrysotile/brake dust exposure group. Using the quantitative evaluation of fibrotic response with confocal microscopy, there was no statistically significant difference trend between the air control group and either the brake dust alone or the brake dust with chrysotile exposure group at any time point through 91 days after cessation of exposure.

The crocidolite asbestos sample used in the study was unique as it was obtained as a commercial crocidolite asbestos sample from the mine such as would have been destined to be shipped to the manufacturing end-user. The crocidolite asbestos produced inflammatory response from day 0 which progressed to Wagner grade 4 interstitial fibrosis within 32 days following cessation of exposure. In addition, the confocal microscopy evaluation of the fibrotic response in the connective tissue showed a linear increase in fibrotic response through 91 days after cessation of exposure. When compared to the air control group at 91 days, the mean level of fibrotic response was 5 times greater. The long crocidolite fibers had a clearance half-time of greater than 1000 days.

There are many brake linings still in use worldwide that contain chrysotile. This study provides in-vivo toxicological support that brake dust derived from chrysotile containing brake drums would not initiate a pathological response in the lung following short term inhalation.

Conflict of interest statement

This study was funded by Honeywell International Inc. The affiliations of the authors are as shown on the cover page and include research laboratories, government institute, corporate affiliations, as well as independent toxicology consultant. This publication is the professional work product of the authors and may not necessarily represent the views of the corporate sponsor. One of the authors, David Bernstein, has appeared as an expert witness in litigation concerned with alleged health effects of exposure to chrysotile. Honeywell is a defendant in asbestos-product litigation and its predecessor manufactured the automotive brakes used in this study. There have been periodic communications between Honeywell and the authors concerning the status of this study. The contribution of Prof JI Phillips is based on research supported by the National Research Foundation.

Appendix A. Supplementary data

Supplementary data to this article can be found online at <http://dx.doi.org/10.1016/j.taap.2014.01.016>.

References

- Antonini, J.M., Charron, T.G., Roberts, J.R., et al., 1999. Application of laser scanning confocal microscopy in the analysis of particle-induced pulmonary fibrosis. *Toxicol. Sci.* 51 (1), 126–134 (Sep).
- Bernstein, D.M., Riego-Sintes, J.M.R., 1999. Methods for the determination of the hazardous properties for human health of man made mineral fibers (MMMF). In: Bernstein, D.M., Riego-Sintes, J.M.R. (Eds.), Vol. EUR 18748 EN, April 93. European Commission Joint Research Centre, Institute for Health and Consumer Protection, Unit: Toxicology and Chemical Substances, European Chemicals Bureau (Available from: <http://ecb.ei.jrc.it/DOCUMENTS/Testing-Methods/mmmfweb.pdf>).
- Bernstein, D.M., Mast, R., Anderson, R., et al., 1994. An experimental approach to the evaluation of the biopersistence of respirable synthetic fibers and minerals. *Environ. Health Perspect.* 102 (Supplement 5), 15–18.
- Bernstein, D.M., Rogers, R., Smith, P., 2003. The biopersistence of Canadian chrysotile asbestos following inhalation. *Inhal. Toxicol.* 15, 101–128.
- Bernstein, D.M., Rogers, R., Smith, P., 2004. The biopersistence of Brazilian chrysotile asbestos following inhalation. *Inhal. Toxicol.* 16, 745–761.
- Bernstein, D.M., Rogers, R., Smith, P., 2005a. The biopersistence of Canadian chrysotile asbestos following inhalation: final results through 1 year after cessation of exposure. *Inhal. Toxicol.* 17, 1–14.
- Bernstein, D.M., Chevalier, J., Smith, P., 2005b. Comparison of Calidria chrysotile asbestos to pure tremolite: final results of the inhalation biopersistence and histopathology following short term exposure. *Inhal. Toxicol.* 17, 427–449.
- Bernstein, D.M., Donaldson, K., Decker, et al., 2008. A biopersistence study following exposure to chrysotile asbestos alone or in combination with fine particles. *Inhal. Toxicol.* 20, 1009–1028.
- Bernstein, D.M., Rogers, R.A., Sepulveda, R., et al., 2010. The pathological response and fate in the lung and pleura of chrysotile in combination with fine particles compared to amosite asbestos following short term inhalation exposure — interim results. *Inhal. Toxicol.* 22, 937–962.
- Bernstein, D.M., Rogers, R.A., Sepulveda, R., et al., 2011. Quantification of the pathological response and fate in the lung and pleura of chrysotile in combination with fine

- particles compared to amosite-asbestos following short-term inhalation exposure. *Inhal. Toxicol.* 23, 372–391.
- Bernstein, D., Dunnigan, J., Hesterberg, T., et al., 2013. Health risk of chrysotile revisited. *Crit. Rev. Toxicol.* 43 (2), 154–183 (Feb).
- Blau, P.J., 2001. Compositions, functions, and testing of friction brake materials and their additives. Oak Ridge National Laboratory report ORNL/TM-2001/64, Oak Ridge, Tennessee.
- Bolton, R.E., Vincent, J.H., Jones, A.D., et al., 1983. An overload hypothesis for pulmonary clearance of UICC amosite fibers inhaled by rats. *Br. J. Ind. Med.* 40, 264–272.
- Bosch, R., 2011. Bosch Automotive Handbook, Updated 8th Edition. Robert Bosch GmbH Bentley Publishers (ISBN-13: 978-0-8376-1686-5).
- Butnor, K.J., Sporn, T.A., Roggli, V.L., 2003. Exposure to brake dust and malignant mesothelioma: a study of 10 cases with mineral fiber analyses. *Ann. Occup. Hyg.* 47 (4), 325–330.
- Cannon, W.C., Blanton, E.F., McDonald, K.E., 1983. The flow-past chamber: an improved nose-only exposure system for rodents. *Am. Ind. Hyg. Assoc. J.* 44 (12), 923–928.
- Cossette, M., Delvaux, P., 1979. Technical evaluation of chrysotile asbestos ore bodies. In: Ledoux, R.C. (Ed.), *Short Course in Mineralogical Techniques of Asbestos Determination*. Mineralogical Association of Canada, Toronto, Canada, pp. 79–109 (May).
- Dodson, R.F., Hammer, S.P., 2012. Asbestos: Risk Assessment, Epidemiology and Health Effects, 2nd edition. CRC Press, Taylor & Francis Group, Boca Raton, Florida.
- EUR 18748 EN, 1999. Methods for the determination of the hazardous properties for human health of man made mineral fibers (MMMF). In: Bernstein, D.M., Riego-Sintes, J.M.R. (Eds.), Vol. EUR 18748 EN, April. 93. European Commission Joint Research Centre, Institute for Health and Consumer Protection, Unit: Toxicology and Chemical Substances, European Chemicals Bureau (<http://ecb.ejrc.it/DOCUMENTS/Testing-Methods/mmmfweb.pdf>).
- Finley, B.L., Pierce, J.S., Paustenbach, D.J., et al., 2012. Malignant pleural mesothelioma in US automotive mechanics: reported vs expected number of cases from 1975 to 2007. *Regul. Toxicol. Pharmacol.* 64 (1), 104–116.
- Freeman, M.D., Kohles, S.S., 2012. Assessing specific causation of mesothelioma following exposure to chrysotile asbestos-containing brake dust. *Int. J. Occup. Environ. Health* 18 (4), 329–336 (Oct–Dec).
- Harper, G.A., 1998. Brakes and Friction Materials: The History and Development of the Technologies. Mechanical Engineering Publications Limited, London, England.
- Hesterberg, T.W., Müller, W.C., Musselman, R.P., et al., 1996. Biopersistence of man-made vitreous fibers and crocidolite asbestos in the rat lung following inhalation. *Fundam. Appl. Toxicol.* 29 (2), 269–279.
- Hesterberg, T.W., Chase, G., Axten, C., et al., 1998. Biopersistence of synthetic vitreous fibers and amosite asbestos in the rat lung following inhalation. *Toxicol. Appl. Pharmacol.* 151 (2), 262–275.
- ILSI, Bernstein, D., Castranova, V., Donaldson, K., et al., 2005. Testing of fibrous particles: short-term assays and strategies. *Inhal. Toxicol.* 17, 497–537.
- Kobell, F., 1834. Ueber den schillernden Asbest von Reichenstein in Schlesien. *J. Prakt. Chem.* 2, 297–298.
- Laden, F., Stampfer, M.J., Walker, A.M., 2004. Lung cancer and mesothelioma among male automobile mechanics: a review. *Rev. Environ. Health* 19 (1), 39–61.
- Lemen, R.A., 2004. Asbestos in brakes: exposure and risk of disease. *Am. J. Ind. Med.* 45 (3), 229–237.
- Lin, L.I.-K., 2000. A note on the concordance correlation coefficient. *Biometrics* 56, 324–325.
- Lin, Lawrence I-Kuei, 1989. A concordance correlation coefficient to evaluate reproducibility. *Biometrics (Int. Biom. Soc.)* 45 (1), 255–268.
- Marsh, G.M., Youk, A.O., Roggli, V.L., 2011. Asbestos fiber concentrations in the lungs of brake repair workers: commercial amphiboles levels are predictive of chrysotile levels. *Inhal. Toxicol.* 23 (12), 681–688.
- McConnell, E.E., Davis, J.M., 2002. Quantification of fibrosis in the lungs of rats using a morphometric method. *Inhal. Toxicol.* 14 (3), 263–272.
- McConnell, E.E., Wagner, J.C., Skidmore, et al., 1984. A comparative study of the fibrogenic and carcinogenic effects of UICC Canadian chrysotile B asbestos and glass microfibre (JM 100). In: *Biological Effects of Man-made Mineral Fibres*. World Health Organization, pp. 234–252.
- Morgan, A., 1995. Deposition of inhaled asbestos and man-made mineral fibers in the respiratory tract. *Ann. Occup. Hyg.* 39 (5), 747–758.
- Morrow, P.E., 1988. Possible mechanisms to explain dust overloading of the lung. *Fundam. Appl. Toxicol.* 10, 369–384.
- Morrow, P.E., 1992. Dust overloading of the lungs: update and appraisal. *Toxicol. Appl. Pharmacol.* 113, 1–12.
- Muhle, H., Bellman, B., Heinrich, U., 1988. Overloading of lung clearance during chronic exposure of experimental animals to particles. *Ann. Occup. Hyg.* 32, 141–147.
- Musselman, R.P., Müller, W.C., Eastes, W., et al., 1994. Biopersistence of man-made vitreous fibers and crocidolite fibers in rat lungs following short-term exposures. *Environ. Health Perspect.* 102 (Suppl. 5), 139–143.
- Oberdörster, G., 1995. Lung particle overload: implications for occupational exposures to particles. *Regul. Toxicol. Pharmacol.* 21, 123–135.
- Osmond-McLeod, M.J., Poland, C.A., Murphy, F., et al., 2011. Durability and inflammogenic impact of carbon nanotubes compared with asbestos fibers. *Part Fiber Toxicol.* 8, 15.
- Paustenbach, D.J., Finley, B.L., Lu, E.T., et al., 2004. Environmental and occupational health hazards associated with the presence of asbestos in brake linings and pads (1900 to present): a “state-of-the-art” review. *J. Toxicol. Environ. Health B Crit. Rev.* 7 (1), 25–80 (Jan–Feb).
- Richter, R.O., Finley, B.L., Paustenbach, D.J., et al., 2009. An evaluation of short-term exposures of brake mechanics to asbestos during automotive and truck brake cleaning and machining activities. *J. Expo. Sci. Environ. Epidemiol.* 19 (5), 458–474 (Jul).
- Rogers, R.A., Antonini, J.M., Brismar, H., et al., 1999. In situ microscopic analysis of asbestos and synthetic vitreous fibers retained in hamster lungs following inhalation. *Environ. Health Perspect.* 107 (5), 367–375 (May).
- Shedd, K.B., 1985. Fiber dimensions of crocidolites from Western Australia, Bolivia, and the Cape and Transvaal Provinces of South Africa. U.S. Bureau of Mines Report of Investigations 8998 United States Department of the Interior.
- Skinner, H.C.W., Ross, M., Frondel, C., 1988. Asbestos and Other Fibrous Materials — Mineralogy, Crystal Chemistry, and Health Effects. Oxford University Press, New York (NY).
- Speil, S., Leineweber, J.P., 1969. Asbestos minerals in modern technology. *Environ. Res.* 2, 166–208.
- StatSoft, Inc., 2011. STATISTICA (data analysis software system), version 12. www.statsoft.com.
- Tanji, T., Yada, K., Akatsuka, Y., 1984. Alternation of clino- and orthochrysotile in a single fiber as revealed by high-resolution electron microscopy. *Clay. Clay Miner.* 32 (5), 429–432 (October 1984).
- Titulaer, M.K., van Miltenburg, J.C., Jansen, J.B.H., et al., 1993. Characterization of tubular chrysotile by thermoporometry, nitrogen sorption, drifts, and TEM. *Clay. Clay Miner.* 41, 496–513.
- VDI Guideline 3492, 2004. Indoor Air Measurement, Ambient Air Measurement, Measurement of Inorganic Fibrous Particles, Scanning Electron Microscopy Method. Verein Deutscher Ingenieure e.V., Düsseldorf.
- Virta, R.L., 2002. Asbestos: Geology, Mineralogy, Mining, and Uses. Prepared in Cooperation with Kirk-Othmer Encyclopedia of Chemical Technology. USGS Open file 02-149, Online Edition. Wiley-Interscience, a division of John Wiley & Sons, Inc., New York (NY).
- Weir, F.W., Meraz, L.B., 2001. Morphological characteristics of asbestos fibers released during grinding and drilling of friction products. *Appl. Occup. Environ. Hyg.* 16 (12), 1147–1149.
- Whittaker, E.J.W., 1957. The structure of chrysotile. V. Diffuse reflexions and fiber texture. *Acta Crystallogr.* 10, 149–156.
- Whittaker, E.J.W., 1960. The crystal chemistry of the amphiboles. *Acta Crystallogr.* 13, 291–298.
- Whittaker, E.J.W., 1963. Research report: Chrysotile fibers — filled or hollow tubes? Mathematical interpretation may resolve conflicting evidence. *Chem. Eng. News* 41, 34–35 (September 30, 1963).
- WHO, 1985. Reference Methods for Measuring Airborne Man-Made Mineral Fibers (MMMF), WHO/EURO MMMF Reference Scheme. World Health Organisation, Copenhagen.